

Draft Final Report
STUDY ACOUSTIC EMISSIONS FROM COMPOSITES

Contract Number: NAS8-38609

Delivery order: 182

Prepared by and Co-Principle Investigator

James L. Walker
Center for Automation and Robotics
University of Alabama in Huntsville
Huntsville, AL 35899
(205)-895-6578*207

Co-Principle Investigator

Gary L. Workman
Center for Automation and Robotics
University of Alabama in Huntsville
Huntsville, AL 35899
(205)-895-6578*240

Submitted to

Chuck Wilkerson
EH13
National Aeronautics and Space Administration
Marshall Space Flight Center, AL 35812
(205)-544-8834

December, 1997

ABSTRACT

The nondestructive evaluation (NDE) of future propulsion systems utilizing advanced composite structures for the storage of cryogenic fuels, such as liquid hydrogen or oxygen, presents many challenges. Economic justification for these structures requires, light weight, reusable components with an infrastructure allowing periodic evaluation of structural integrity after enduring demanding stresses during operation. A major focus has been placed on the use of acoustic emission NDE to detect propagating defects, in service, necessitating an extensive study into characterizing the nature of acoustic signal propagation at very low temperatures and developing the methodology of applying AE sensors to monitor cryogenic components.

This work addresses the question of sensor performance in the cryogenic environment. Problems involving sensor mounting, spectral response and durability are addressed. The results of this work provides a common point of measure from which sensor selection can be made when testing composite components at cryogenic temperatures.

TABLE OF CONTENTS

1.0 INTRODUCTION	4
2.0 EXPERIMENTAL	5
3.0 RESULTS	7
4.0 SENSOR PERFORMANCE TESTING AT -440° F	13
5.0 TENSILE TESTING AT -320° F	13
6.0 CONCLUSIONS.....	15
7.0 APPENDICES	16
APPENDIX A Summary of Cryogenic Tests	16
APPENDIX B Sensor Activity During Long Term Exposure To LH ₂	19
APPENDIX C Sensor Activity During Cooldown	20
APPENDIX D Signals Before Cryogenic Cycling	30
APPENDIX E Signals After Second Cryogenic Cycle	37
APPENDIX F Signals After fifth Cryogenic Cycle	45

1.0 INTRODUCTION

Three questions arise when applying AE analysis to a loaded structure in a cryogenic environment. First, how do the sensors react to the cryogenic environment. Secondly, how does the cryogenic environment effect the acoustic propagation characteristics in the composite and sensor couplant. Lastly, how does the composite material behave at cryogenic temperatures. The first of these questions is answered in this report by conducting a series of tests to characterize how acoustic emission sensors perform when subjected to a cryogenic environment. The later two point are works in progress and will be appended to this report as they are completed.

Several commercially available sensors were selected for this study based upon availability, size and frequency response. The application of AE to large composite fuel tanks, anticipated for future launch systems, would involve many sensors (50+), to provide adequate coverage in what is a highly attenuative material. Due to the limited space available for mounting sensors and the weight restrictions on a launch vehicle, the size of the sensors are very important during sensor selection. The frequency response bandwidth of the chosen sensor would need to be in the range of 100 kHz to 2.0 Mhz to ensure that the signals from the various failure modes in the composite were detected.

Each sensor used in this study went though a series of cryogenic tests involving exposure to temperatures down to approximately -320 °F, the nominal temperature of liquid nitrogen “LN₂”. Of particular interest was the amount and nature of the acoustic activity generated by the sensors as they cooled to the cryogenic temperature and then warmed back up to ambient conditions. The survivability of each sensor to thermal cycling was tested over ten thermal cycles from room temperature (nominally 75 °F) to -320 °F and back to room temperature. Also, of interest was how the cryogenic environment affected sensor performance. Here, the sensors were pulsed from a common source as they cooled and the amplitude and spectral response recorded. In this manner the fidelity of each sensor could be checked and compared between themselves and at various temperatures.

2.0 EXPERIMENTAL

In all, twelve sensors were thermally cycled for this study. A summary of the manufacturer, size, and construction of each sensor is given in Table 1. Each sensor was pulsed from a common 5.0 Mhz ultrasonic sensor. Here, an eighteen inch long, half inch diameter 6061 -T6 aluminum rod was used as a wave guide and the sensors and pulser were bonded with hot melt glue. After establishing the reference condition of each sensor it was tested for cumulative activity and frequency response variations during cool down.

Table 1. Sensors tested.

Manufacturer	Model	S/N	Diameter (inch)	Cable	Location	Wear Plate
Harisonic	HAE-1004	M10056	0.40	Microdot	End	Ceramic
Harisonic	CM-0204	J12050	0.40	Microdot	End	Ceramic
Digital Wave	B-1025	944240	0.43	Microdot	Side	Ceramic
PAC	R15	AL78	0.69	Microdot	Side	Ceramic
PAC	R30	302	0.69	Microdot	Side	Ceramic
PAC	S9208	AC36	1.00	Microdot	Side	Metal
PAC	WD	AC81	0.69	Differential	Side	Ceramic
PAC	S9215	AB53	0.75	BNC	Side	Metal
PAC	R15-T1	AA01	0.69	Microdot	Top	Ceramic
PAC	R15-T2	AA02	0.69	Microdot	Top	Ceramic
PAC	Mini-30	AB50	0.40	BNC	Top	Ceramic
PAC	Nano-30	AA02	0.25	BNC	Top	Ceramic

PAC = Physical Acoustics Corporation

The primary intent of the first phase of testing was to determine how the sensors react to a cryogenic environment. That is, what signals are generated by the sensors alone as they cool from normal room temperature to near liquid nitrogen temperatures. To accomplish this task, the sensors were suspended by their lead wire in a beaker submerged in a liquid nitrogen bath (Figure 1). The air temperature from the bottom of the beaker to just below the nitrogen level was measured with a thermocouple to be in the range of -320° F. The acoustic emission system was configured for continuous operation and the sensors were suspended one at a time near the bottom of the inner beaker and monitored for 30 to 60 minutes. Lead breaks (0.5 mm HB) were performed on the sides of the beaker and cross support holding the sensor to determine if the boil off of the LN₂ along the outside of the inner beaker created any measurable AE at the sensor position. None of the lead breaks were received by the AE system verifying that the only signals recorded would be from the sensors themselves encountering a thermal gradient. After completing the chill down cycle the AE system was paused and the sensor remove from the nitrogen container. The AE system was restarted and left to run for 10 additional minutes so that the warm-up emissions could be recorded. This process was repeated for a total of ten cryogenic cycles or until the sensor failed to operate. Appendix A outlines the ten cryogenic tests.

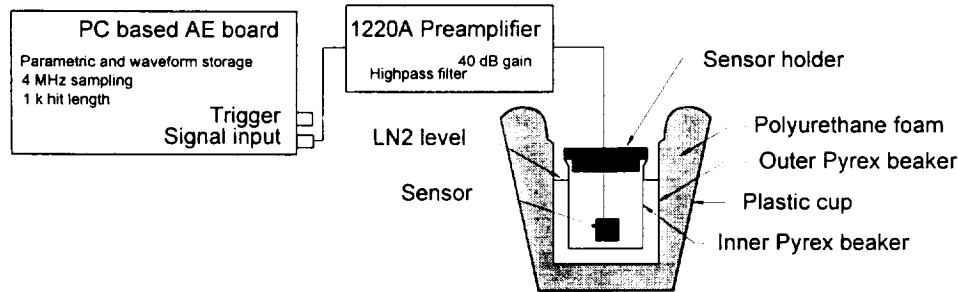


Figure 1. Configuration to measure sensor activity during cool down.

The second phase of this project involved measuring sensor performance during cool down and at cryogenic temperatures. Here the reference frequency response was compared to the response curves generated for each sensor as it cooled to LN₂ levels and stabilized. As in the initial sensor check-out tests, an 18 inch aluminum rod was used as a waveguide between the 5.0 Mhz pulser and test AE sensor. The rod was held vertically over the cryogenic container with the AE sensor positioned just off the bottom of the inner “chilled” beaker (Figure 2). The receiving sensor was bonded with a proprietary cryogenic tolerant adhesive while the pulser was attached with hot melt glue. In this manner a common excitation signal could be received and compared between sensors at various points in the cool down cycle. An acousto-ultrasonic style system was incorporated to take these measurements. The system fired the pulser; recorded the signal from the AE sensor and computed the subsequent power spectrum. Measurements were taken at room temperature and then every 15 minutes over the one hour cool down, for a total of five measurements.

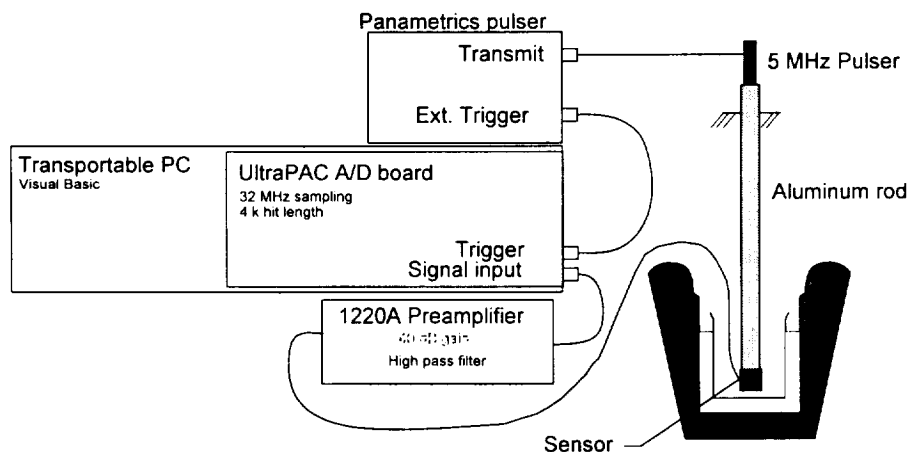


Figure 2. Configuration for pulse test during cool down.

3.0 RESULTS

The sensors were compared based upon activity during cool down, activity during warm up, time to the first 10% of cumulative activity, time to 90% of cumulative activity, stability between cycles and cycle life. Overall acoustic activity during cool down would indicate the amount of data that would have to be filtered out after a cryogenic structural test. The time to 10% and 90% of cumulative activity would provide a measure of the event rate and settling time for each sensor. Finally, the stability between cycles and cycle life of the sensor can tell which sensors are rugged enough to be used in a cryogenic environment.

As shown in Table 2 and Figure 3, the overall noisiest three sensors during cool down were the CM-0204 (2669 signals) followed by the HAE-1004 (1994 signals) and the B-1025 (1617 signals). On the other side of the spectrum the quietest three sensors during cool down were the S9208 (170 signals) then the WD (489 signals) and mini-30 (592). The nature of these signals will be described later, but the sheer magnitude of AE activity indicates that for most practical testing situations it will not be practical to record AE activity during cool down. Not only will it be difficult to separate the sensor noise AE from the material activity, the rate of noise related activity may interfere with good signal collection. In other words, the high noise signal rate will increase the probability that mixed material and noise AE signals will be collected as single source events.

Table 2. Sensor activity

Sensor I.D.	Cumulative activity during cool down	Sensor I.D.	Time to 10% Maximum	Sensor I.D.	Time to 90% Maximum
S9208	170	B-1025	19	B-1025	356
WD	489	CM-0204	51	Nano-30	422
Mini-30	592	HAE-1004	84	CM-0204	432
Nano-30	797	Nano-30	93	Mini-30	454
R15	978	WD	89	HAE-1004	661
R30	1253	Mini-30	150	S9208	760
R15-t2	1343	R15T-2	180	R15T-1	795
R15-t1	1562	S9215	194	R15T-2	801
S9215	1616	R15	196	R30	943
B-1025	1617	R30	198	R15	1015
HAE-1004	1994	R15T-1	220	WD	1146
CM-0204	2669	S9208	265	S9215	1219

After the sensors had reached thermal equilibrium at -320 F, the data collection system was paused and the sensors removed from the inner beaker. The AE system was then allowed to continue acquiring data during the warm-up. In general, very little AE activity was recorded during the warm-up, and after approximately 5 minutes at room temperature no additional activity was recorded for any of the sensors. Overall, less than 10% of the cumulative activity recorded during the entire test, cool down and warm-up, was recorded during the warm-up period. The noisiest three sensors during the warm-up period were the WD, S9208 and B-1025 sensors. The quietest sensors were the Nano-30 followed by the HAE-1004 and CM-0204, all with less than 0.3% activity during the warm-up period.

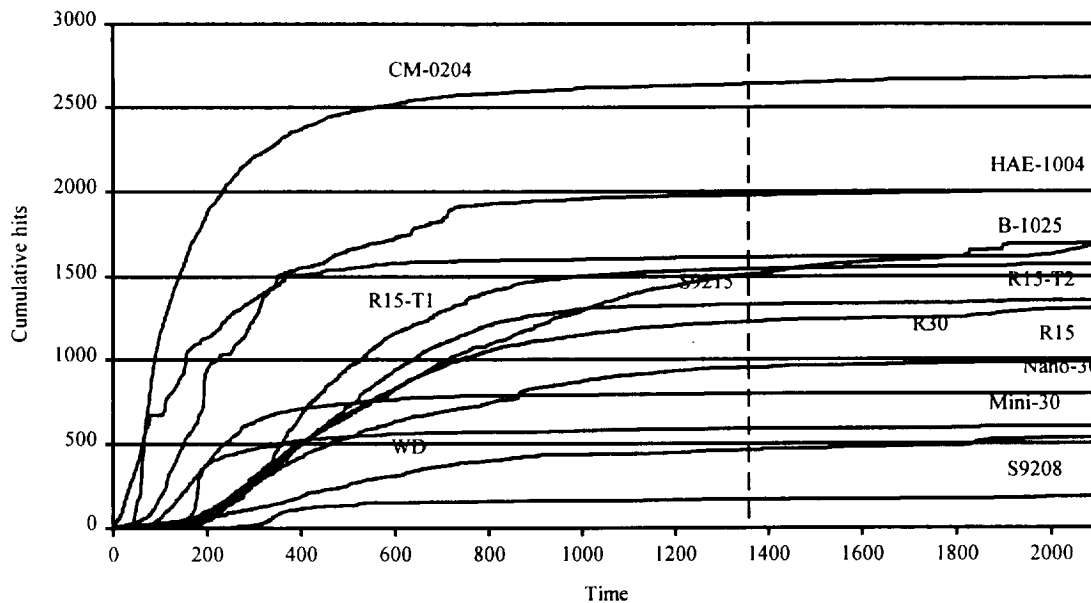


Figure 3. Sensor activity during first cycle cool down to -320 °F.

By observing the second activity plot (Figure 4), one can see that each sensor responds to the cool down at a slightly different rate. The time when the activity has reached 10% and 90% allows provides an indication of the time required to wait after exposing the sensors to a cryogenic environment before the majority of AE recorded is known not to come from the sensor itself cooling down. These times thus provide a measure of how long AE measurements would need to be paused as the structure cools down before data acquisition could begin. The B-1025 sensor stabilized the quickest (356 seconds) of all the sensors tested followed by the Nano-30 (422 seconds) and the CM-0204 (432 seconds). The longest settling time of the sensors came from the S9215, which took over 20 minutes to begin to level out. The WD and R15 were also slow taking over 17 minutes to stabilize. A summary of the settling times for each system is provided in Table 3. A long term exposure test (1 hour) confirmed that little activity was produced after the initial cooldown and that after approximately 45 minutes no appreciable activity was produced (Appendix B)

The characteristics of each sensor over the ten cryogenic cycles was fairly repeatable. No appreciable changes in the frequency, amplitude or energy content of the signals were noted. There was a slight decrease in the cumulative AE activity with cycling, but as shown in Figure 5, the amount of AE generated between cryogenic varied greatly enough that a trend could not be established for all sensors. Overall, no more than a 10% decrease in signal activity was present for any of the sensors tested. Appendix C summarizes the activity rates for each sensor during the ten cryogenic cycles.

Only two of the sensors tested failed during the cryogenic cycling. The HAE-1004 sensor failed after the second cycle while the B-1025 sensor failed after the fifth cycle. In both cases the wear

plate on the sensor face shattered and debonded from the sensor. In general the features of the AE activity covered the entire spectrum which would make it difficult to post filter the data to eliminate the signals originating from the cool down. Classically the most descriptive features used to describe an AE signal is its amplitude, energy and frequency spectrum. Typical amplitude histograms and energy versus amplitude plots are shown in Figures 6 and 7 for the first cool down test.

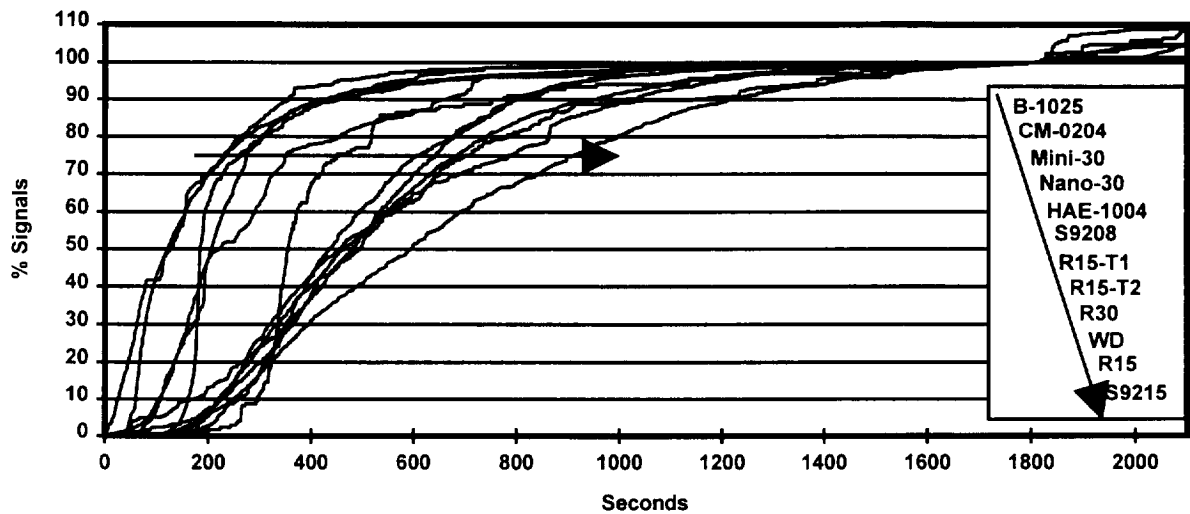


Figure 4. Sensor activity during first cycle cool down to -320 °F.

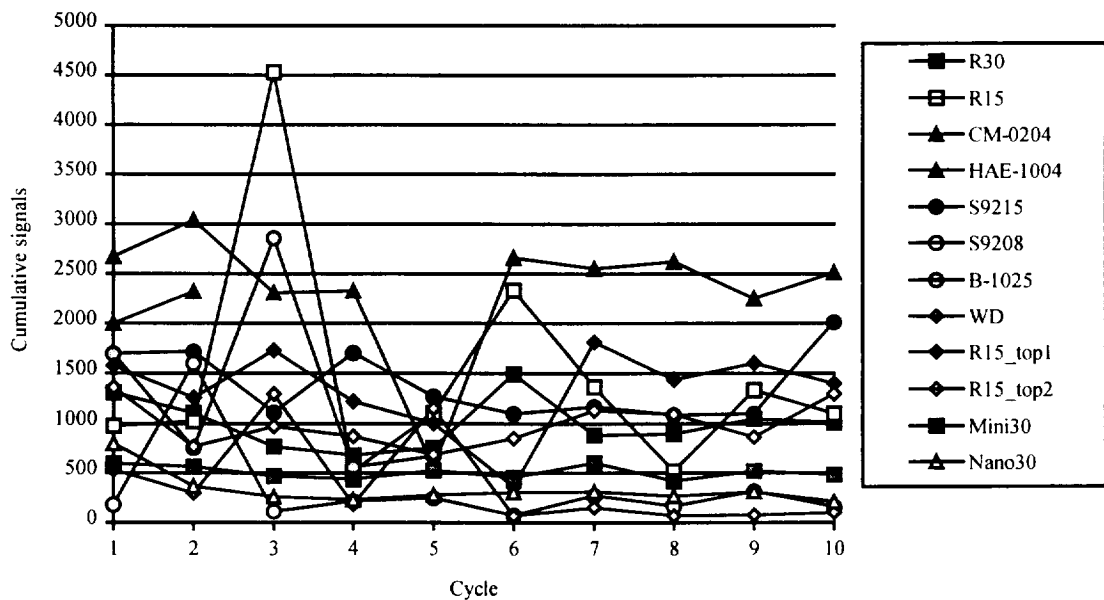


Figure 5. Sensor activity over ten cryogenic cycles

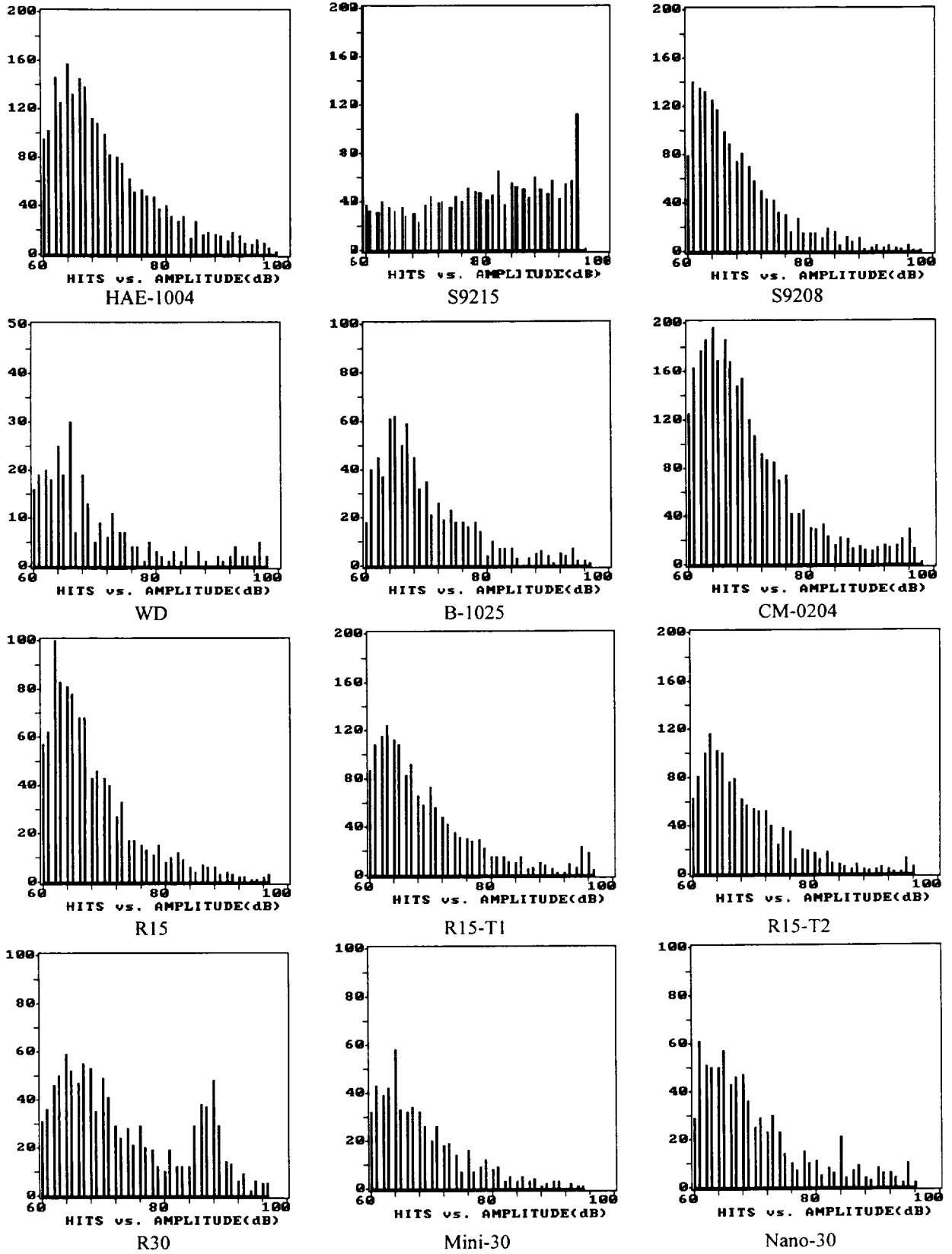


Figure 6. Sensor amplitude distributions during cool down to LN_2 .

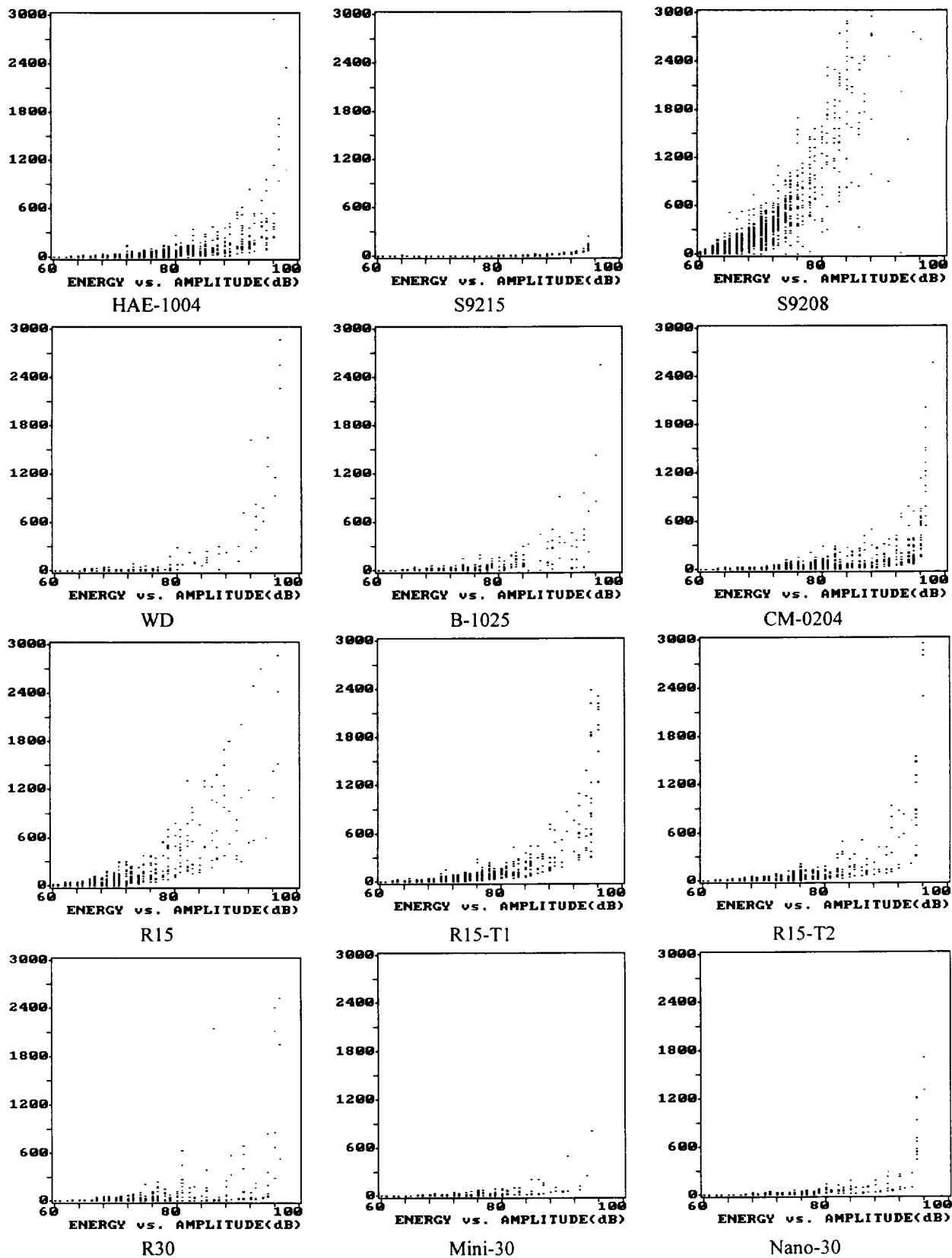


Figure 7. Sensor energy/amplitude distributions during cool down to LN_2 .

During the second phase of sensor testing the effect the cryogenic environment had on the fidelity of each sensor was measured. Here, each AE sensor was pulsed with a common signal the subsequent reaction recorded. In general, there were no observable or noteworthy changes in the resonance peaks as the sensors cooled. In fact, as shown in Figure 8, the relative amount of signal energy increased for the resonant peaks when the sensors were coldest. An additional benefit of this characteristic is that if sensor spacing is determined at room temperature then adequate coverage is guaranteed at cryogenic temperatures. The signals and power spectra for each sensor at their reference condition as well as after two and five cryogenic cycles are provided in Appendix D through E.

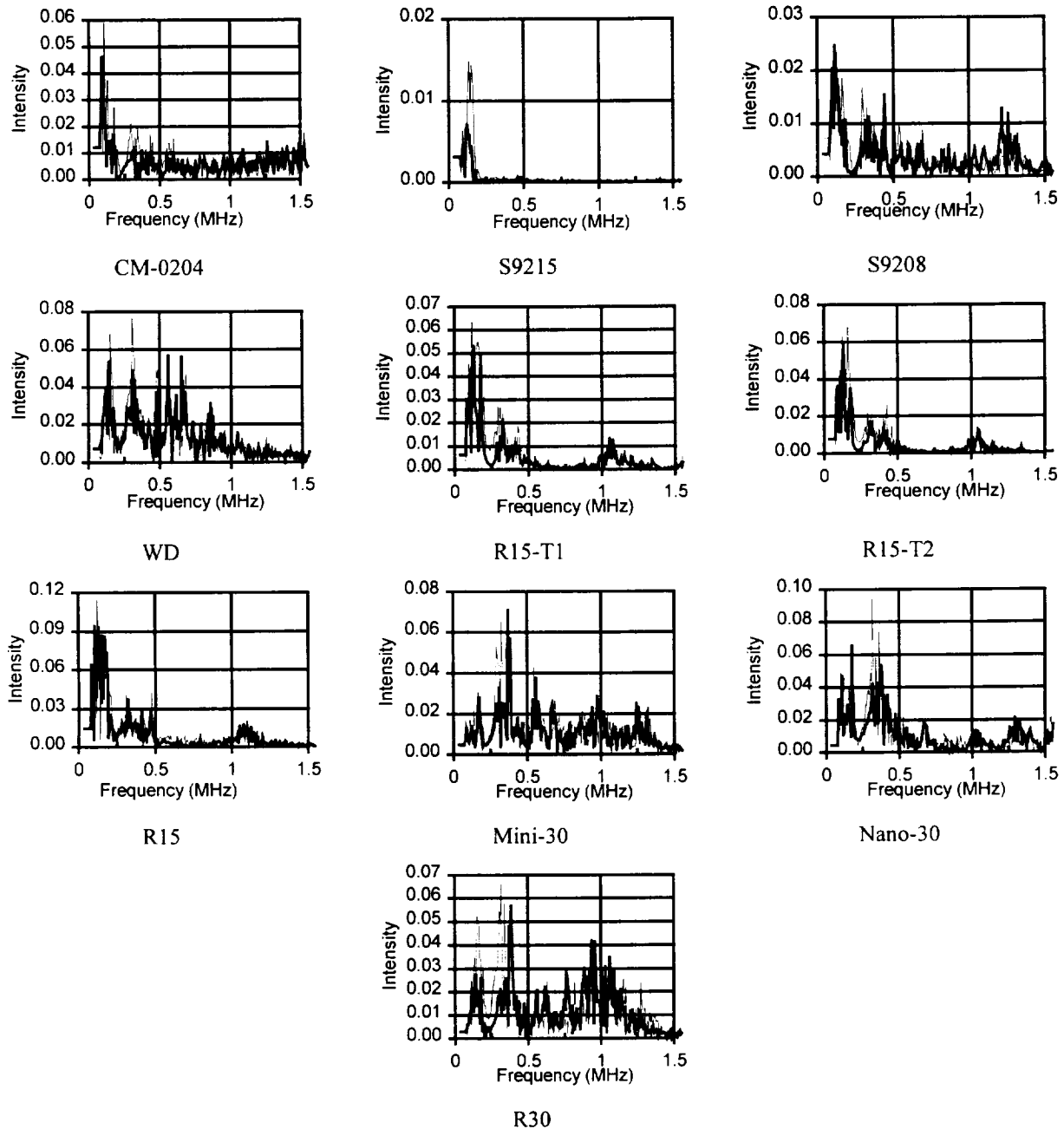


Figure 8. Spectral response comparison (75 °F dark to -320 °F light).

4.0 SENSOR PERFORMANCE TESTING AT -440° F

A series of tests were planned for testing the sensors at approximately -440° F, the temperature of liquid helium. At these temperatures special hardware is necessary to contain and transport liquid helium due to its narrow operational temperature range. The facilities to handle the LH₂ were to be made available through MSFC's Space Sciences Division. The hardware to support the transducers was designed and fabricated at UAH.

Due to scheduling conflicts and difficulty in acquiring the necessary hardware this portion of the task has not been completed. Now though, with all the hardware in place, the helium tests should be able to be completed in a timely manner. When the testing is completed the results will be appended to this report.

5.0 TENSILE TESTING AT -320° F

The process of tensile testing a composite sample while submerged in a cryogenic fluid meant the development of a specialized "wet grip". The grip serves to hold one end of the composite sample while that end is submerged in LN₂ and is attached to the activation ram of a hydraulic tensile testing machine. A schematic of the grip system is shown in Figure 9 and 10.

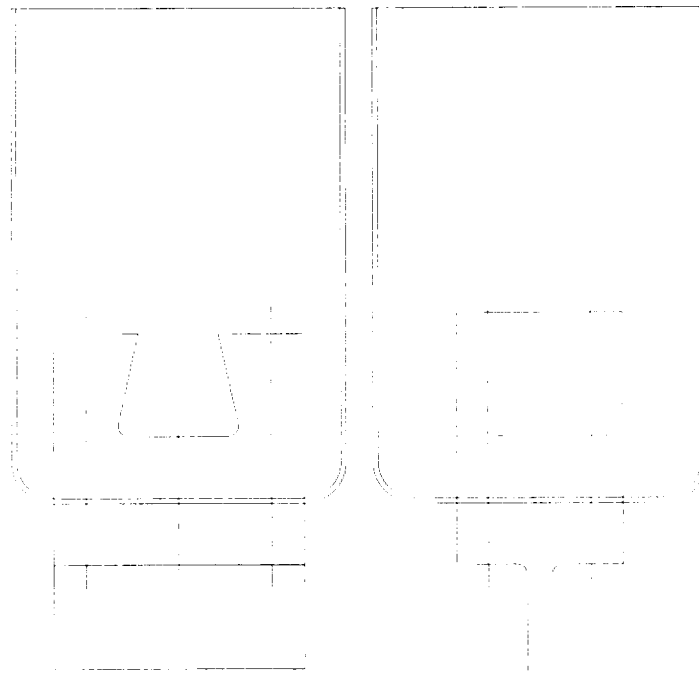
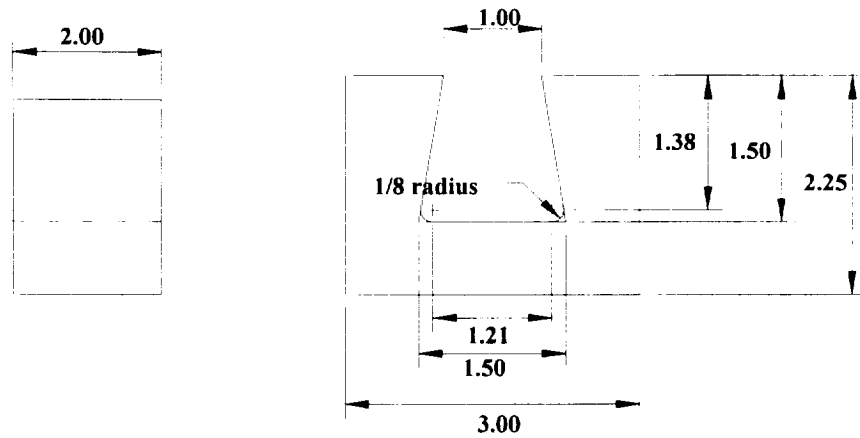
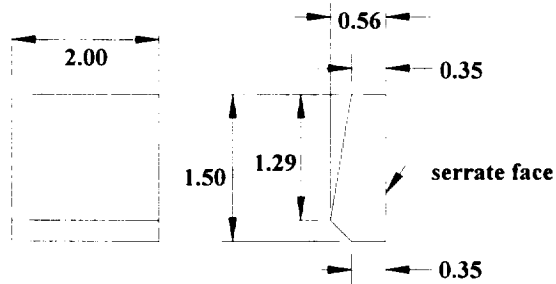


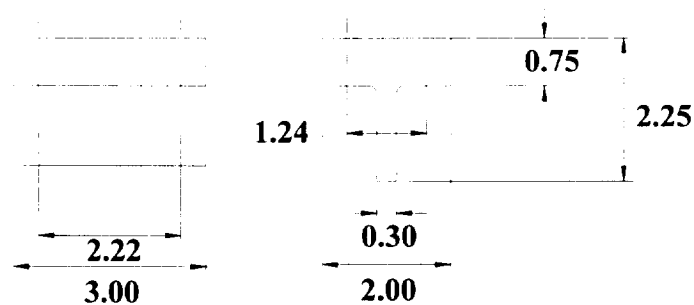
Figure 9. Cryogenic grip



Holder



Grip (2 required)



Attach base

Figure 10. Breakdown of cryogenic grip.

The grip mechanism has just recently been completed and is now undergoing stress testing to ensure that it will not fail during operation. Testing of composite samples will begin shortly and the results appended to this report.

6.0 CONCLUSIONS

The sensor tests addressed in this report have shown that there are several commercially available sensors rugged enough and have sufficient fidelity to be used during AE testing in a cryogenic environment. In general, the sensor activity during cool down begins to stabilize after approximately 10 minutes and reaches an insignificant level after 45 minutes at cryogenic (-320 °F) temperatures. As expected, the larger the sensor, the longer it takes to stabilize and lower the initial activity rate due to the larger thermal mass.

The nature of the AE activity recorded during cool down covers a broad range of parametric and spectral (frequency) values. Post filtering of this data based upon simple amplitude, energy or frequency filters may not be possible. To ensure that the cryogenic signals from the sensors are not recorded as material AE one will most likely have to wait until the sensor thermally stabilizes with the structure or devise some method of prechilling the sensors before the structure is thermally or mechanically loaded.

The performance of the sensors appears to be similar in the cryogenic environment as at room temperature. The signals recorded by the sensors and their subsequent power spectra remain unchanged during the cool down. The only noticeable difference is a slight increase in the energy of the signals at cryogenic temperatures. It is not known at this time whether the increase in energy is solely attributable to the sensor or some function of the waveguide being supercooled.

7.0 APPENDICES

APPENDIX A Summary of Cryogenic Tests

Test 1

Filename	Sensor	Schedule	Hits	Date
R30T004	R30	30 cool down + 5 warm-up	1310	1/31/97
R15TR01	R15	30 cool down	978	1/31/97
R15TR02	R15	5 warm-up	7	1/31/97
RCM01	CM-0204	30 cool down + 5 warm-up	2677	1/31/97
RHEA01	HAE-1004	30 cool down + 5 warm-up	1999	1/31/97
RP01	S9215	30 cool down + 5 warm-up	1699	2/3/97
RS01	S9208	30 cool down + 5 warm-up	184	2/3/97
RDW01	B-1025	30 cool down + 5 warm-up	1695	2/3/97
RWD01	WD	30 cool down + 5 warm-up	533	2/3/97
AA01A01	R15T_1	30 cool down + 5 warm-up	1573	4/11/97
AA02A01	R15T_2	30 cool down + 5 warm-up	1357	4/11/97
Mini01	Mini-30	30 cool down + 5 warm-up	600	4/11/97
Nano01	Nano-30	30 cool down + 5 warm-up	798	4/11/97

Test 2

R30T005	R30	30 cool down + 5 warm-up	1104	2/3/97
R15TR03	R15	30 cool down + 5 warm-up	1026	2/3/97
RCM02	CM-0204	30 cool down + 5 warm-up	3035	2/3/97
RHEA02	HAE-1004	30 cool down + 5 warm-up	2323	2/3/97
RP03	S9215	30 cool down + 5 warm-up	1716	2/10/97
RS03	S9208	30 cool down + 5 warm-up	1601	2/3/97
RDW02	B-1025	30 cool down + 5 warm-up	756	2/3/97
RWD02	WD	30 cool down + 5 warm-up	299	2/3/97
AA01A02	R15T_1	30 cool down + 5 warm-up	1256	4/11/97
AA02A02	R15T_2	30 cool down + 5 warm-up	766	4/11/97
Mini02	Mini-30	30 cool down + 5 warm-up	568	4/11/97
Nano02	Nano-30	30 cool down + 5 warm-up	366	4/11/97

Test 3

R30T008	R30	30 cool down + 5 warm-up	770	2/10/97
R15TR06	R15	30 cool down + 5 warm-up	4532	2/10/97
RCM03	CM-0204	30 cool down + 5 warm-up	2315	2/10/97
RP05	S9215	30 cool down + 5 warm-up	1113	2/12/97
RS05	S9208	30 cool down + 5 warm-up	114	2/12/97
RDW03	B-1025	30 cool down + 5 warm-up	2860	2/10/97
RWD03	WD	30 cool down + 5 warm-up	1298	2/10/97
AA01A03	R15T_1	60 cool down + 10 warm-up	1725/1751	4/11/97
AA02A03	R15T_2	60 cool down + 10 warm-up	970/1202	4/11/97
Mini03	Mini-30	60 cool down + 10 warm-up	450/467	4/14/97
Nano03	Nano-30	60 cool down + 10 warm-up	258/306	4/14/97

Test 4

R30T009	R30	30 cool down + 5 warm-up	682	2/12/97
R15TR07	R15	30 cool down + 5 warm-up	517	2/12/97
RCM04	CM-0204	60 cool down + 10 warm-up	2330/	2/12/97
RP06	S9215	60 cool down + 10 warm-up	1704/	2/19/97
RS06	S9208	30 cool down + 5 warm-up	218	2/12/97
RDW04	B-1025	30 cool down + 5 warm-up	556	2/12/97
RWD04	WD	30 cool down + 5 warm-up	186	2/19/97
AA01A04	R15T_1	30 cool down + 5 warm-up	1218	4/14/97
AA02A04	R15T_2	30 cool down + 5 warm-up	871	4/14/97
Mini04	Mini-30	30 cool down + 5 warm-up	439	4/14/97
Nano04	Nano-30	30 cool down + 5 warm-up	231	4/14/97

Test 5

R30T010	R30	60 cool down + 10 warm-up	753/	2/20/97
R15TR08	R15	60 cool down + 10 warm-up	1104/	2/20/97
RCM06	CM-0204	30 cool down + 5 warm-up	568	2/19/97
RP07	S9215	30 cool down + 5 warm-up	1269	2/20/97
RS08	S9208	60 cool down + 10 warm-up	246/	2/20/97
RDW05	B-1025	60 cool down + 10 warm-up	675/	2/20/97
RWD07	WD	60 cool down + 10 warm-up	1151/	2/25/97
AA01A05	R15T_1	30 cool down + 5 warm-up	1003	4/14/97
AA02A05	R15T_2	30 cool down + 5 warm-up	689	4/14/97
Mini05	Mini-30	30 cool down + 5 warm-up	526	4/15/97
Nano05	Nano-30	30 cool down + 5 warm-up	281	4/14/97

Test 6

Filename	Sensor	Schedule	Hits	Date
R30T011	R30	30 cool down + 5 warm-up	1491	2/28/97
R15TR10	R15	30 cool down + 5 warm-up	2337	2/28/97
RCM07	CM-0204	30 cool down + 5 warm-up	2661	2/28/97
RP08	S9215	30 cool down + 5 warm-up	1098	2/28/97
RS09	S9208	30 cool down + 5 warm-up	77	2/28/97
RWD08	WD	30 cool down + 5 warm-up	73	2/28/97
AA01A06	R15T_1	30 cool down + 5 warm-up	362	4/15/97
AA02A06	R15T_2	30 cool down + 5 warm-up	851	4/15/97
Mini06	Mini-30	30 cool down + 5 warm-up	459	4/15/97
Nano06	Nano-30	30 cool down + 5 warm-up	308	4/16/97

Test 7

R30T013	R30	30 cool down + 5 warm-up	880	2/28/97
R15TR11	R15	30 cool down + 5 warm-up	1366	2/28/97
RCM08	CM-0204	30 cool down + 5 warm-up	2551	2/28/97
RP09	S9215	30 cool down + 5 warm-up	1168	2/28/97
RS10	S9208	30 cool down + 5 warm-up	272	2/28/97
RWD09	WD	30 cool down + 5 warm-up	153	2/28/97
AA01A07	R15T_1	30 cool down + 5 warm-up	1812	4/16/97
AA02A07	R15T_2	30 cool down + 5 warm-up	1129	4/16/97
Mini07	Mini-30	30 cool down + 5 warm-up	603	4/16/97
Nano07	Nano-30	30 cool down + 5 warm-up	310	4/16/97

Test 8

R30T014	R30	30 cool down + 5 warm-up	897	3/1/97
R15TR12	R15	30 cool down + 5 warm-up	518	3/2/97
RCM09	CM-0204	30 cool down + 5 warm-up	2624	3/2/97
RP10	S9215	30 cool down + 5 warm-up	1088	3/2/97
RS11	S9208	30 cool down + 5 warm-up	167	3/2/97
RWD10	WD	30 cool down + 5 warm-up	67	3/2/97
AA01A08	R15T_1	30 cool down + 5 warm-up	1436	4/16/97
AA02A08	R15T_2	30 cool down + 5 warm-up	1093	4/16/97
Mini08	Mini-30	30 cool down + 5 warm-up	417	4/16/97
Nano08	Nano-30	30 cool down + 5 warm-up	264	4/16/97

Test 9

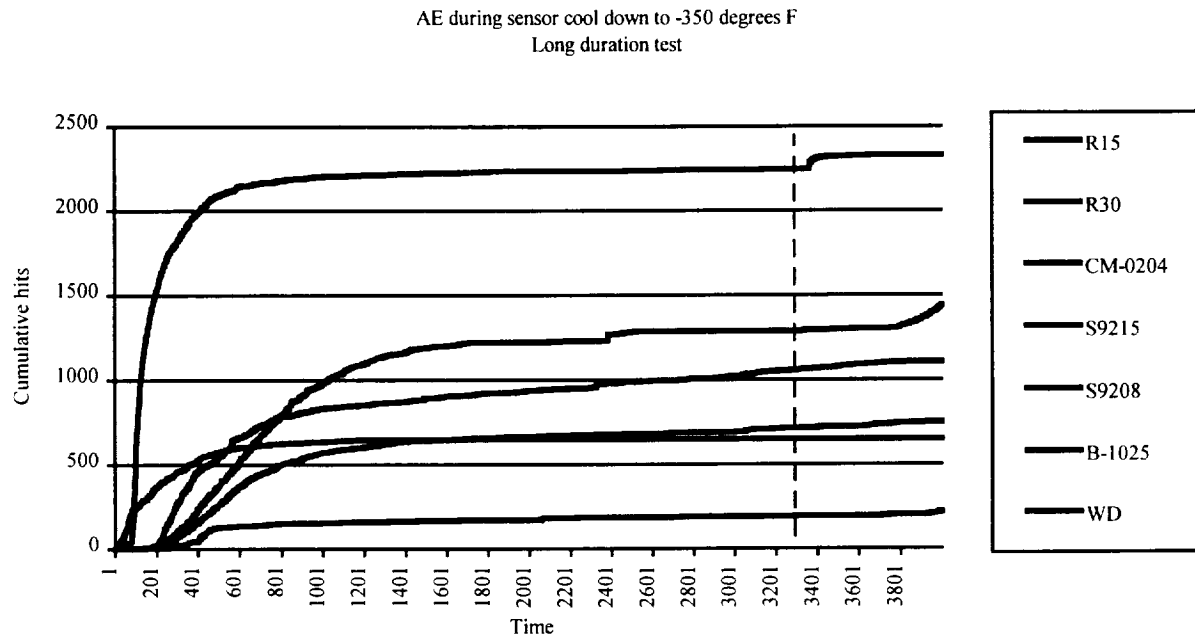
R30T015	R30	30 cool down + 5 warm-up	1046	3/3/97
R15TR14	R15	30 cool down + 5 warm-up	1337	3/3/97
RCM10	CM-0204	30 cool down + 5 warm-up	2258	3/3/97
RP11	S9215	30 cool down + 5 warm-up	1096	3/3/97
RS12	S9208	30 cool down + 5 warm-up	315	3/3/97
RWD11	WD	30 cool down + 5 warm-up	76	3/3/97
AA01A09	R15T_1	30 cool down + 5 warm-up	1603	4/16/97
AA02A09	R15T_2	30 cool down + 5 warm-up	867	4/16/97
Mini09	Mini-30	30 cool down + 5 warm-up	524	4/17/97
Nano09	Nano-30	30 cool down + 5 warm-up	310	4/17/97

Test 10

R30T016	R30	30 cool down + 5 warm-up	1013	3/4/97
R15TR16	R15	30 cool down + 5 warm-up	1098	3/4/97
RCM11	CM-0204	30 cool down + 5 warm-up	2514	3/4/97
RP12	S9215	30 cool down + 5 warm-up	2011	3/4/97
RS13	S9208	30 cool down + 5 warm-up	160	3/4/97
RWD12	WD	30 cool down + 5 warm-up	103	3/4/97
AA01A10	R15T_1	30 cool down + 5 warm-up	1397	4/17/97
AA02A10	R15T_2	30 cool down + 5 warm-up	1295	4/17/97
Mini10	Mini-30	30 cool down + 5 warm-up	480	4/17/97
Nano10	Nano-30	30 cool down + 5 warm-up	212	4/17/97

APPENDIX B

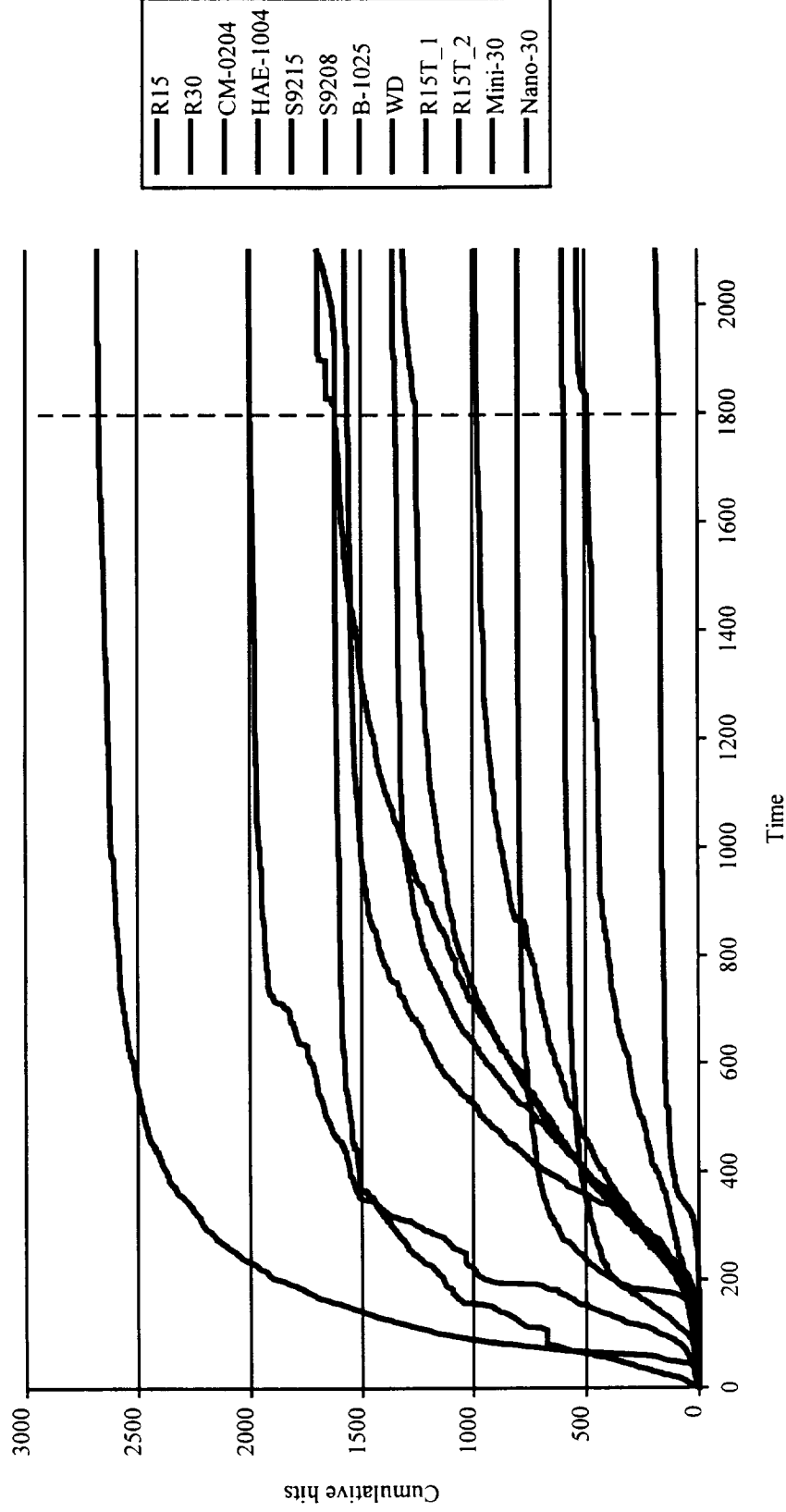
Sensor Activity During Long Term Exposure to LH₂



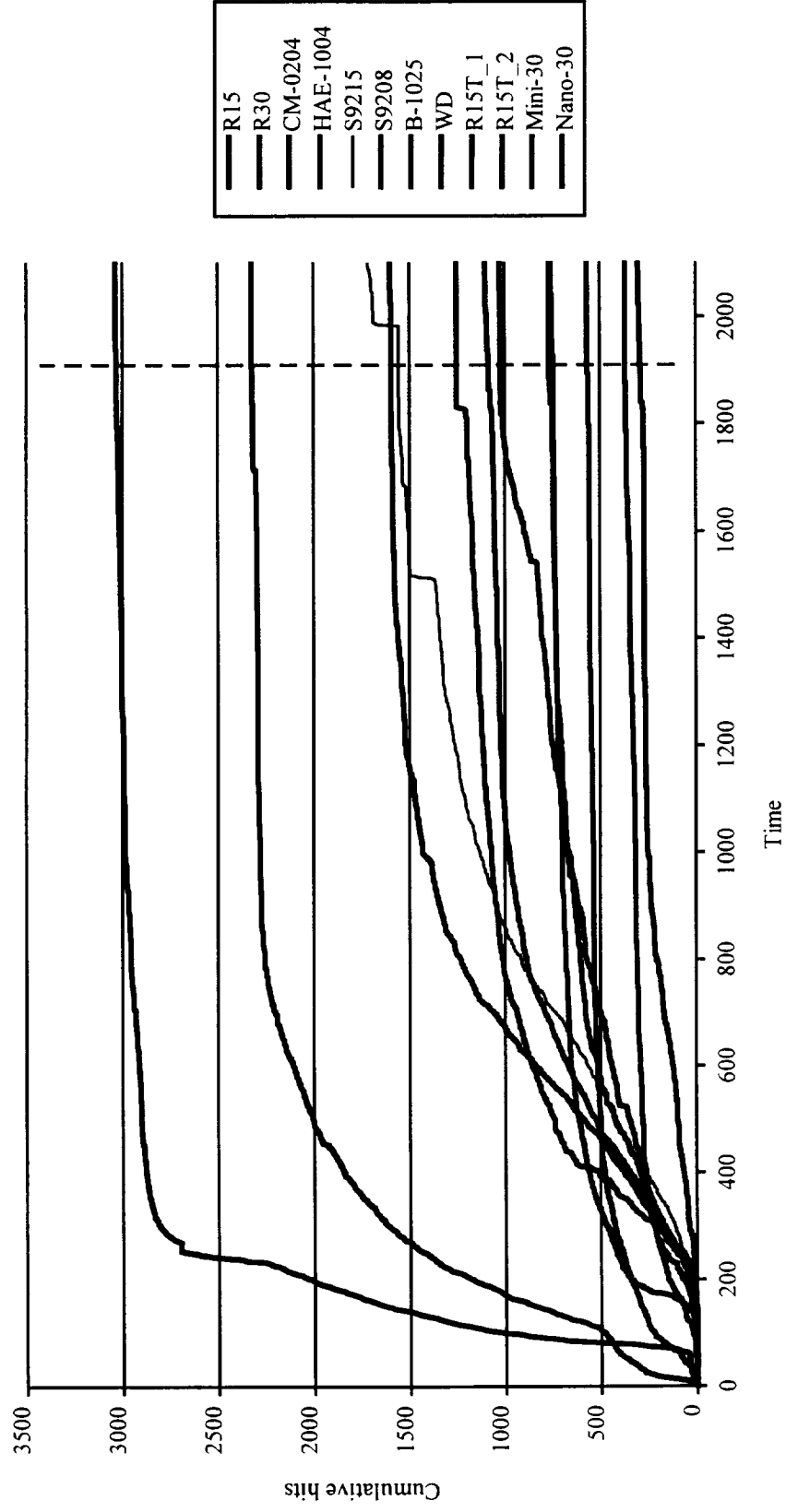
APPENDIX C

SENSOR ACTIVITY DURING COOLDOWN

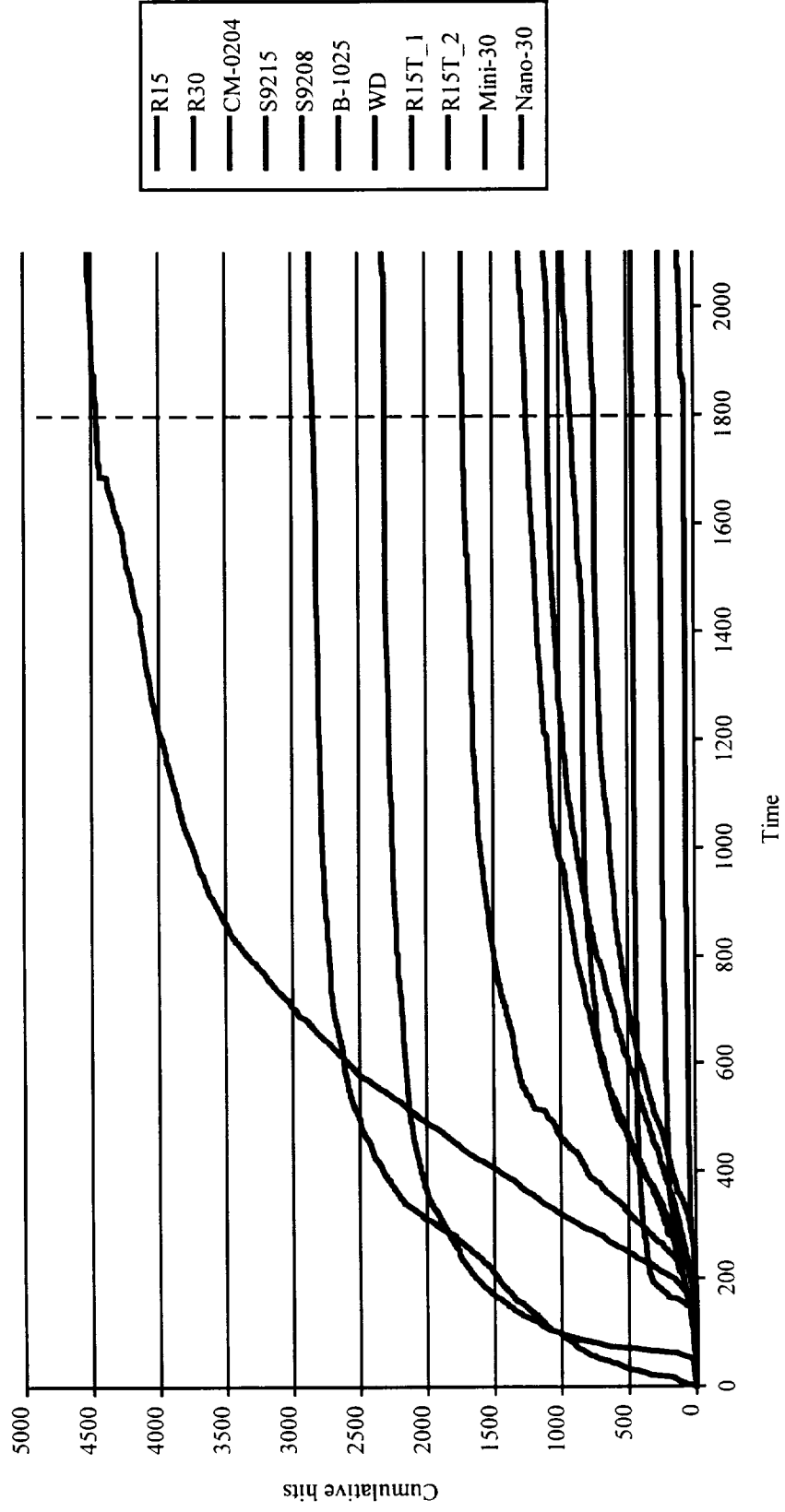
AE during sensor cool down to -350 degrees F
Test 1



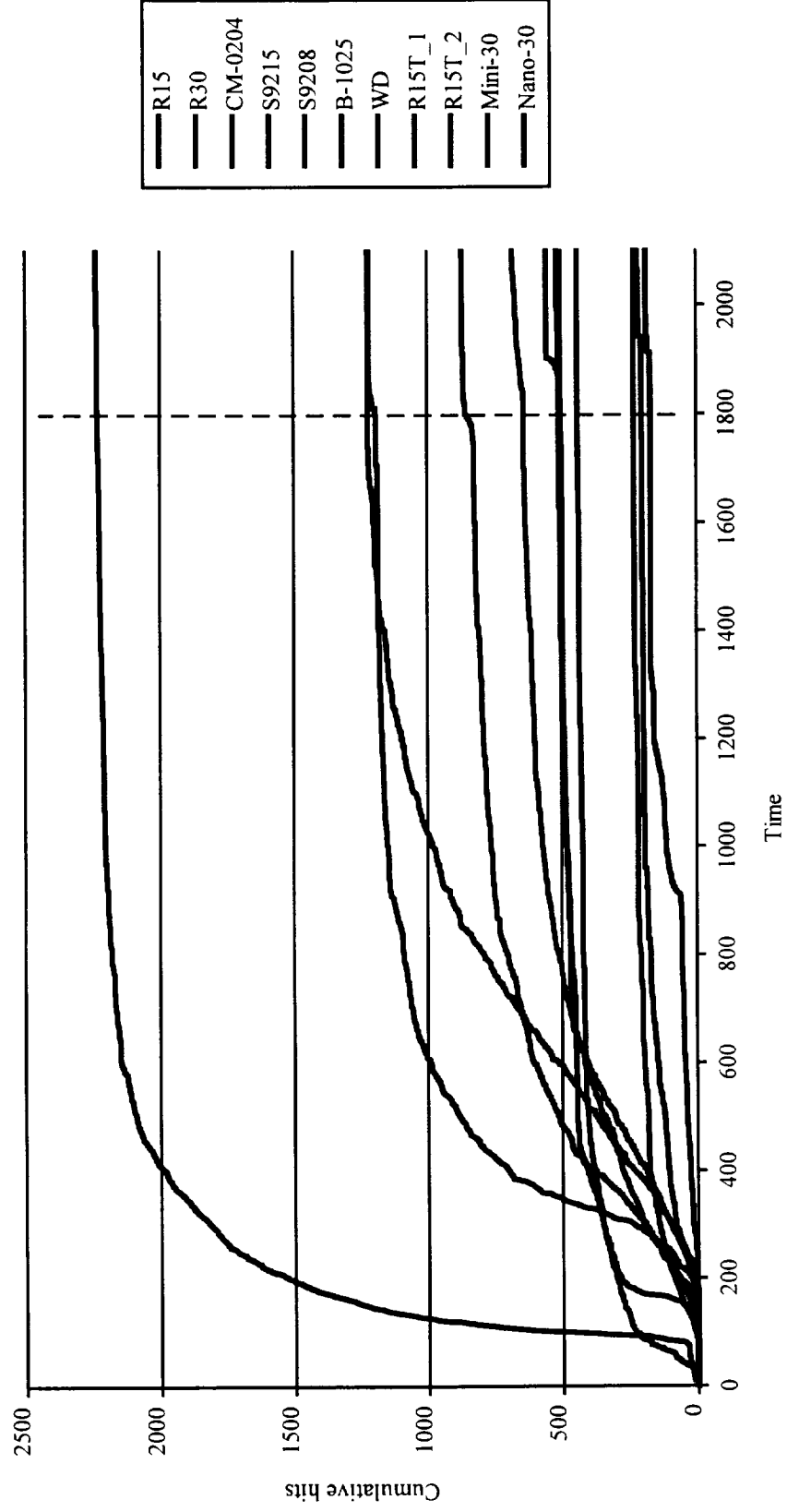
AE during sensor cool down to -350 degrees F
Test 2



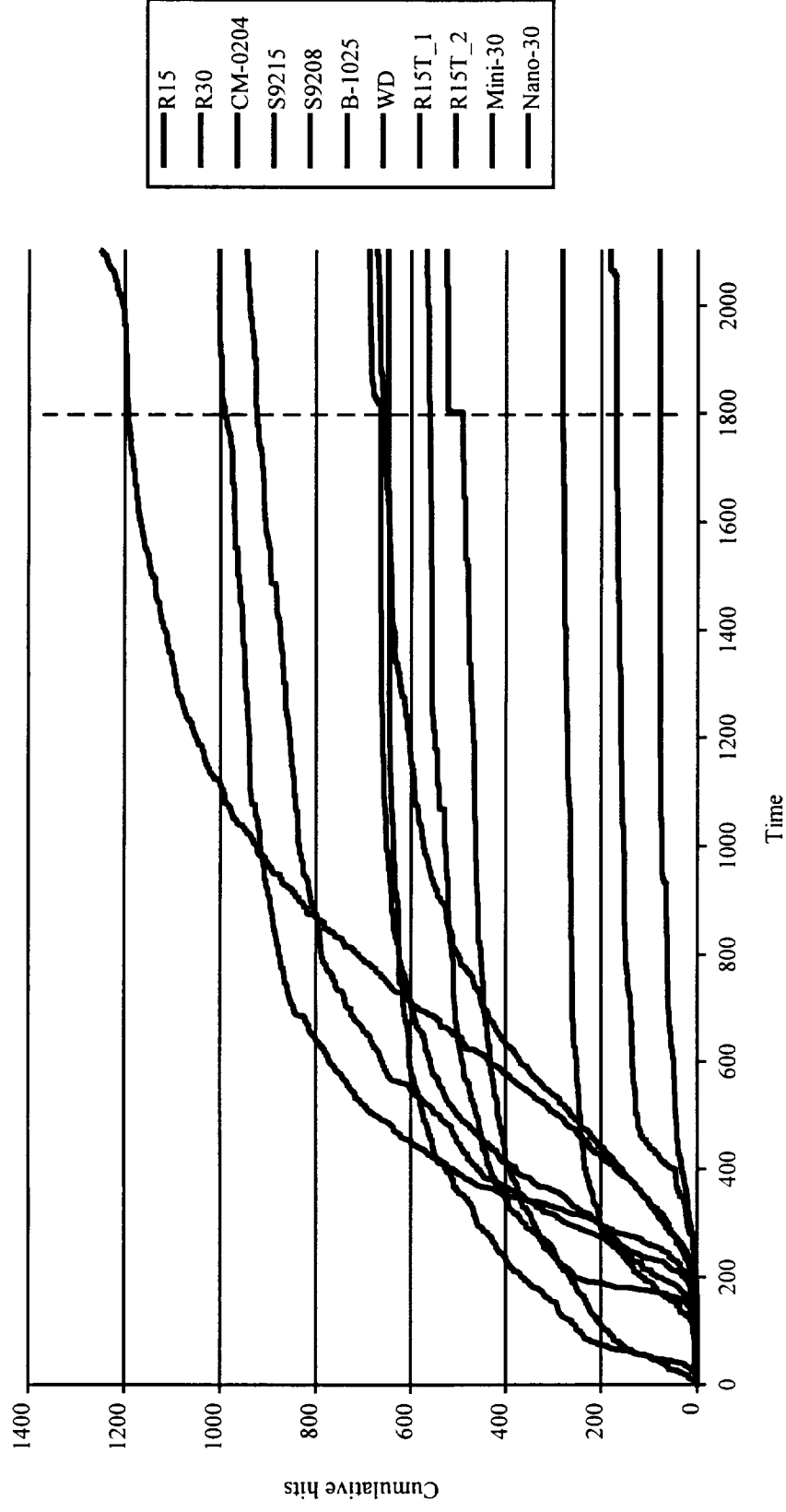
AE during sensor cool down to -350 degrees F
Test 3



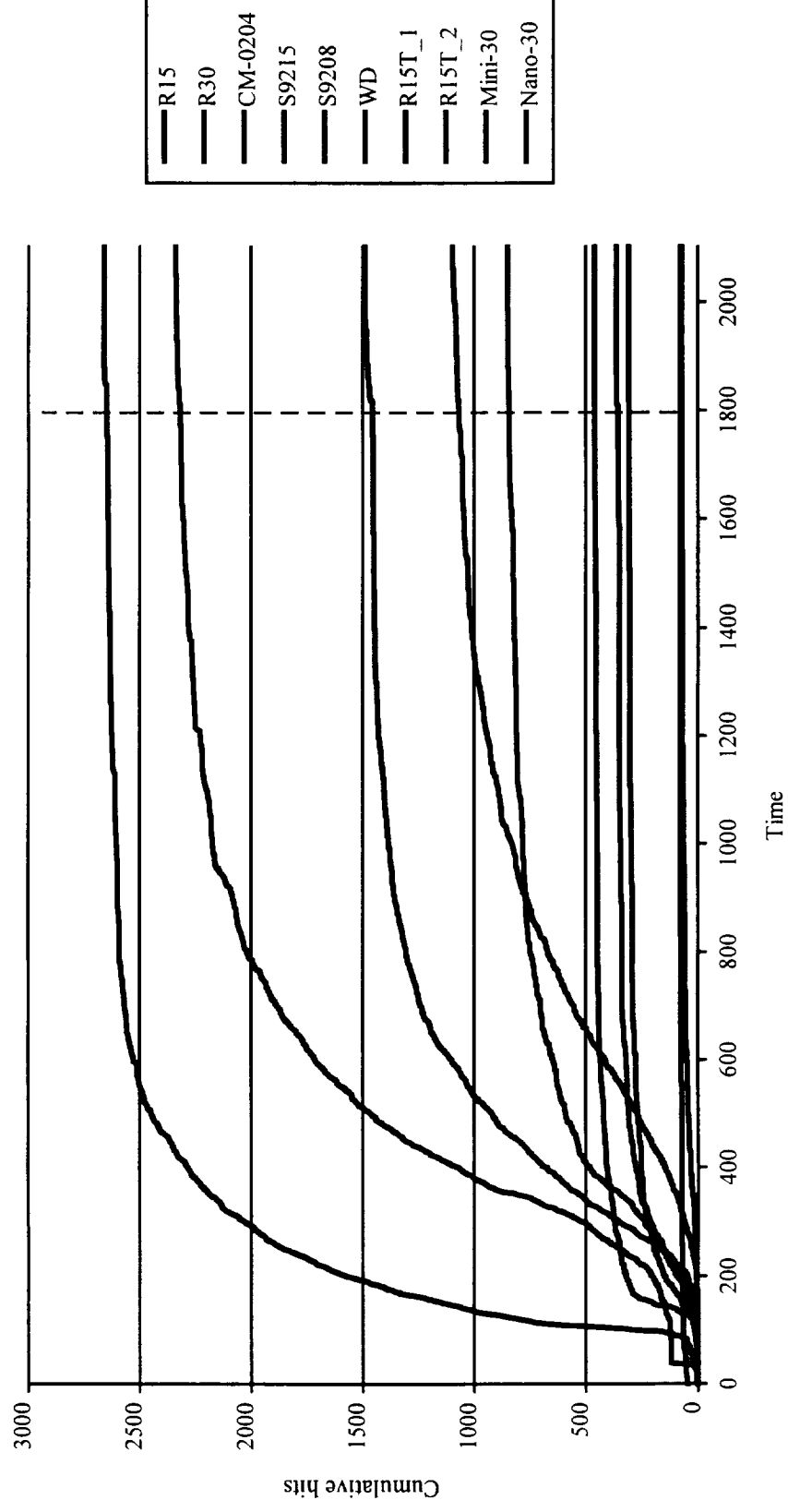
AE during sensor cool down to -350 degrees F
Test 4



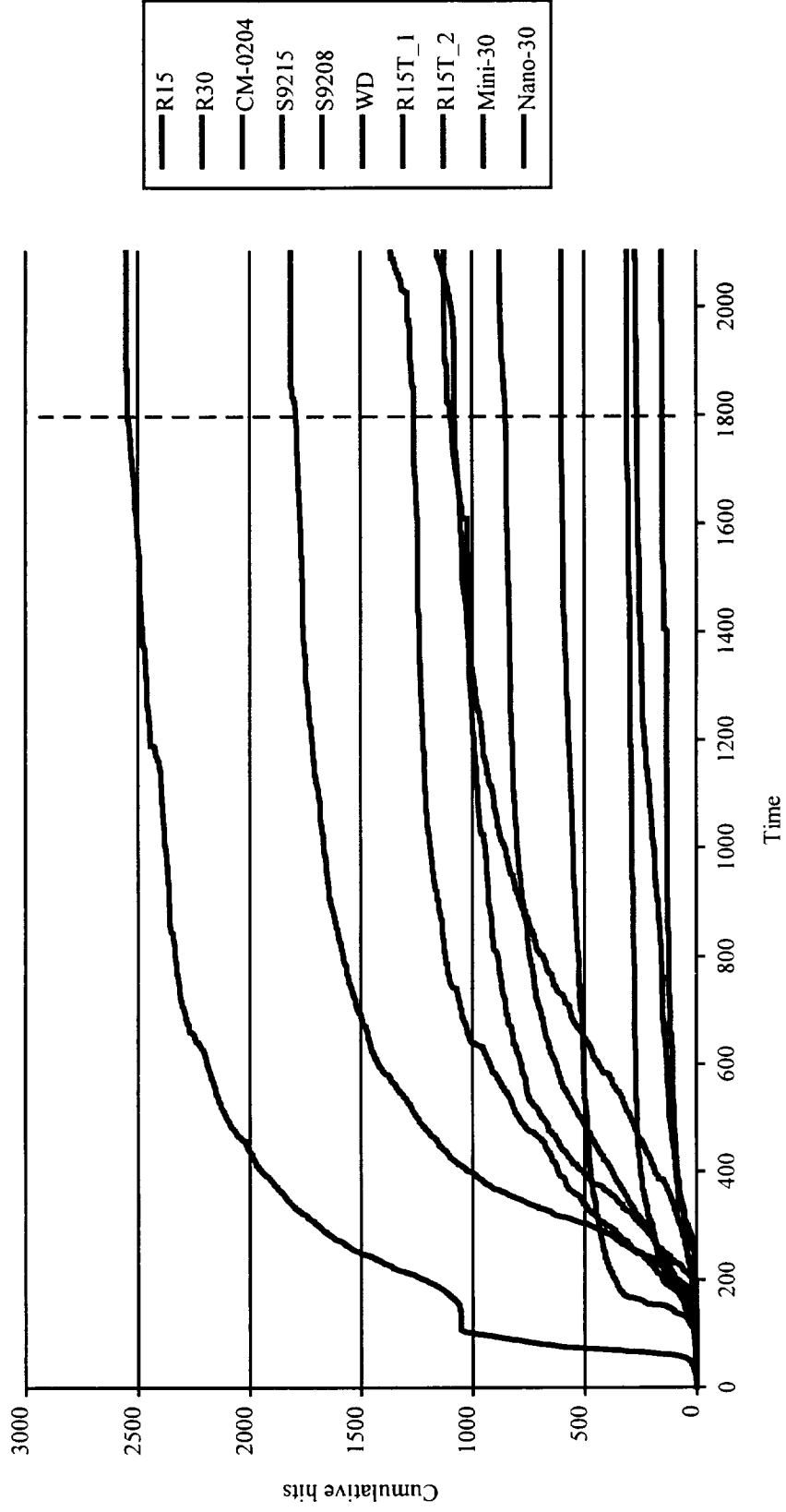
AE during sensor cool down to -350 degrees F
Test 5



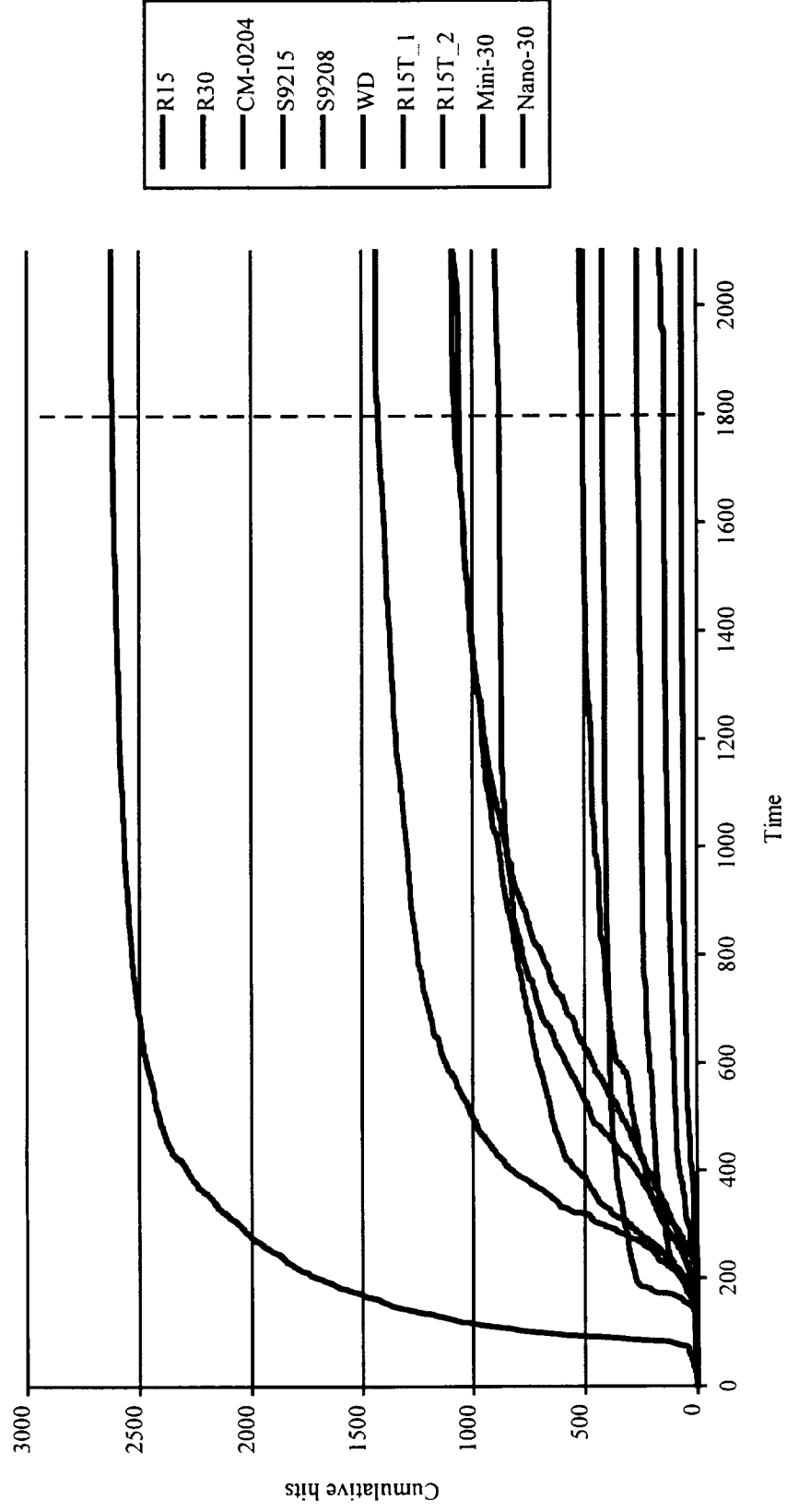
AE during sensor cool down to -350 degrees F
Test 6



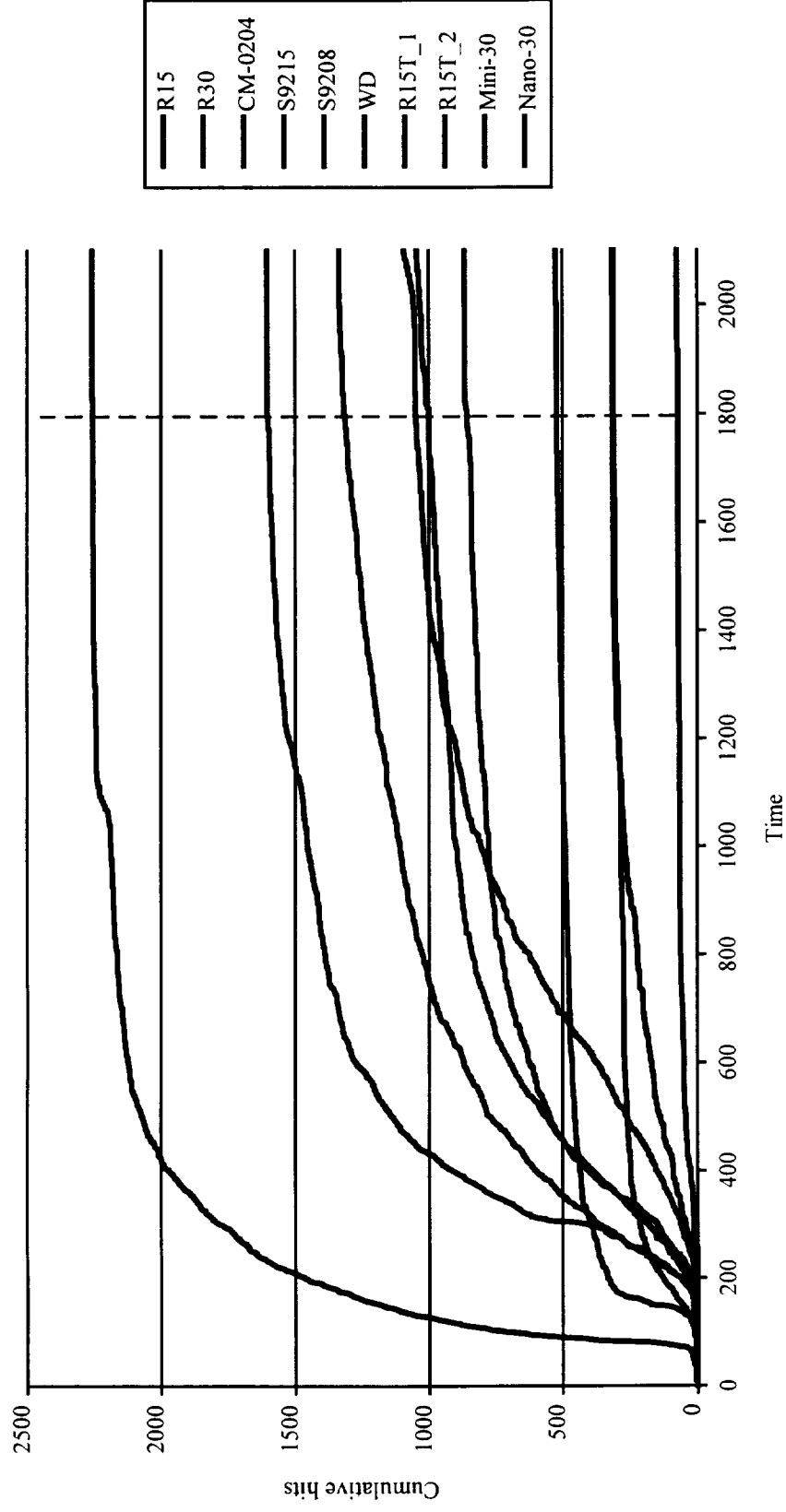
AE during sensor cool down to -350 degrees F
Test 7



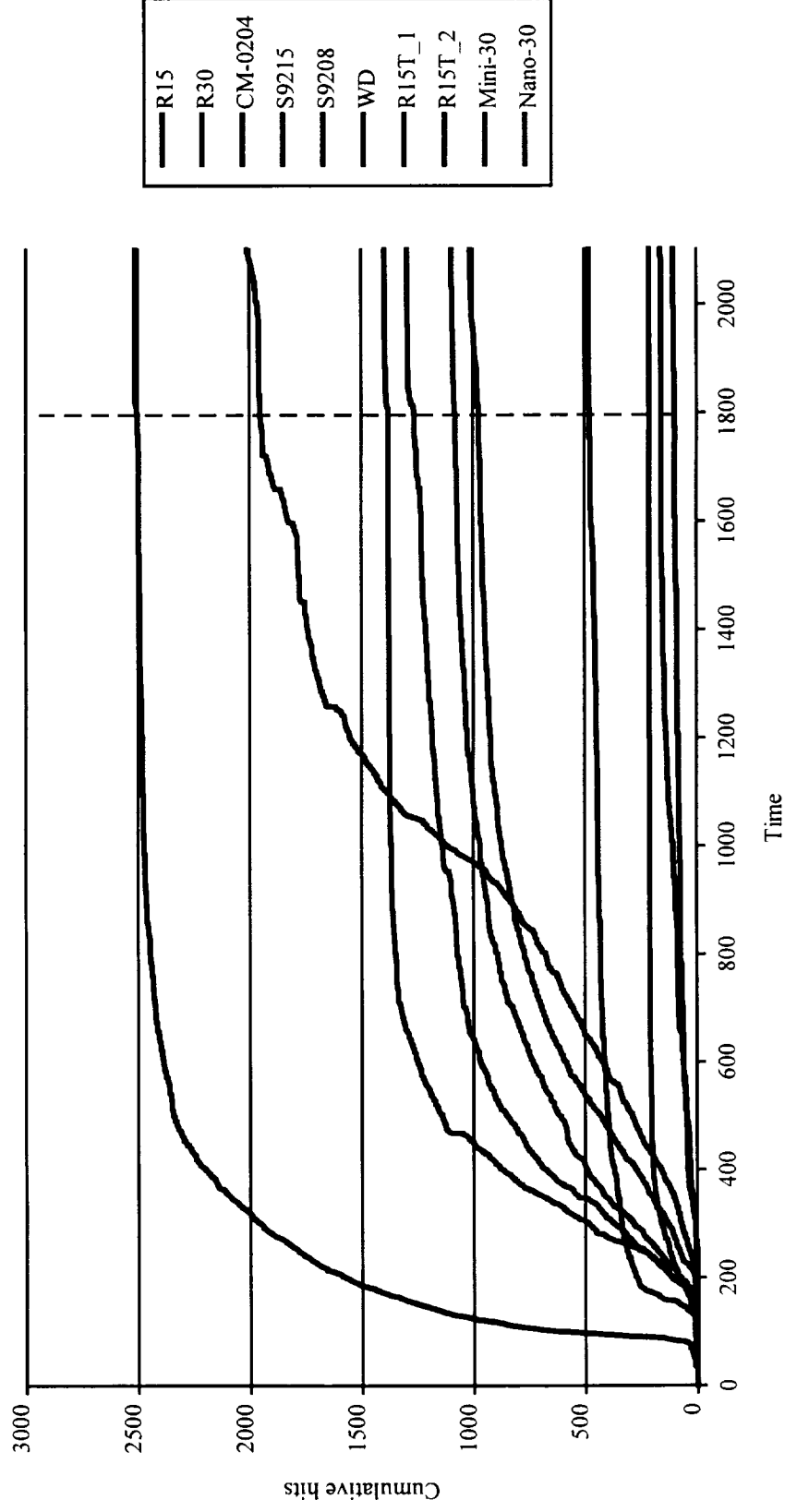
AE during sensor cool down to -350 degrees F
Test 8



AE during sensor cool down to -350 degrees F
Test 9



AE during sensor cool down to -350 degrees F
Test 10

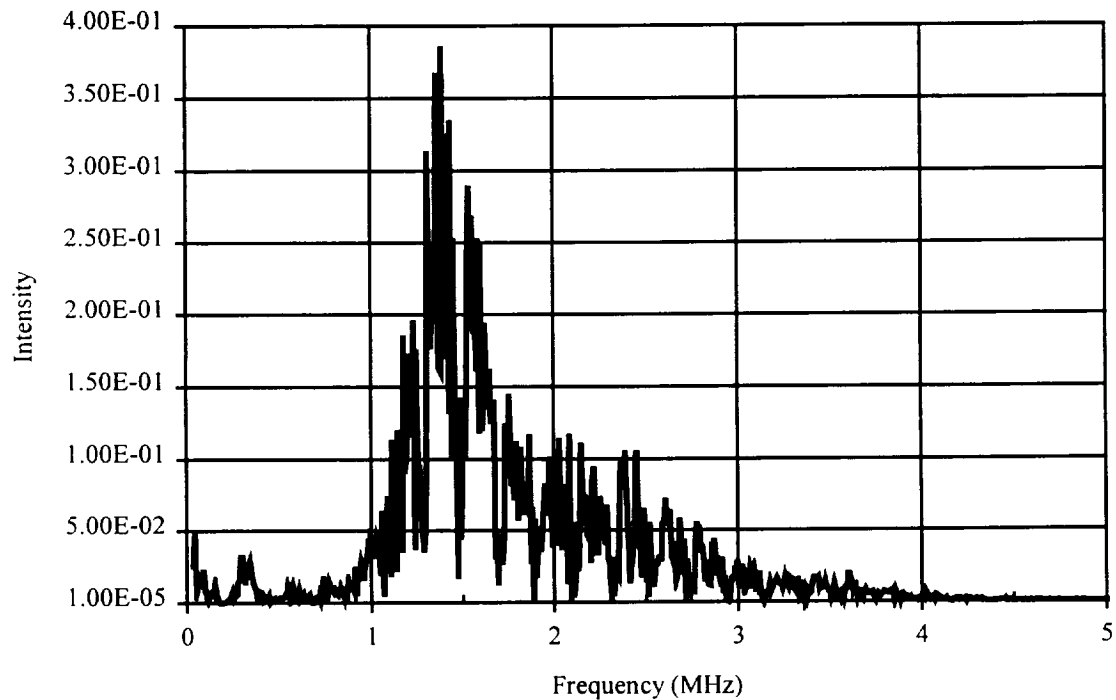
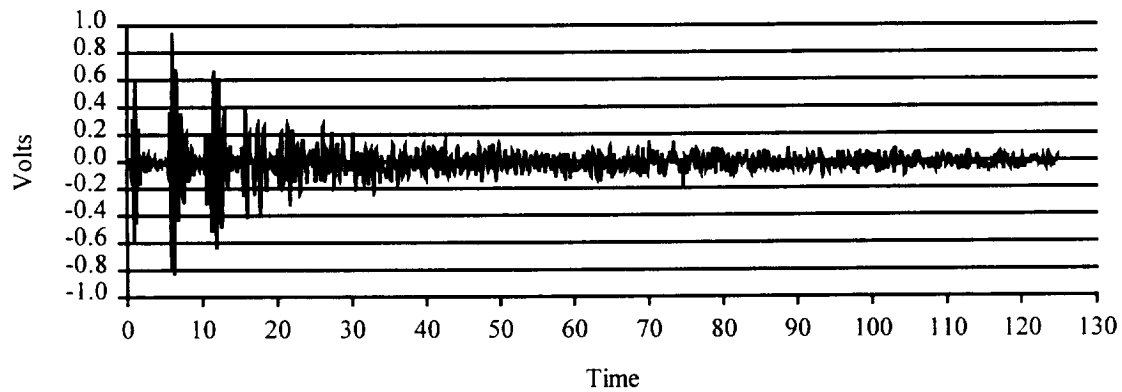


APPENDIX D SIGNALS BEFORE CRYOGENIC CYCLING

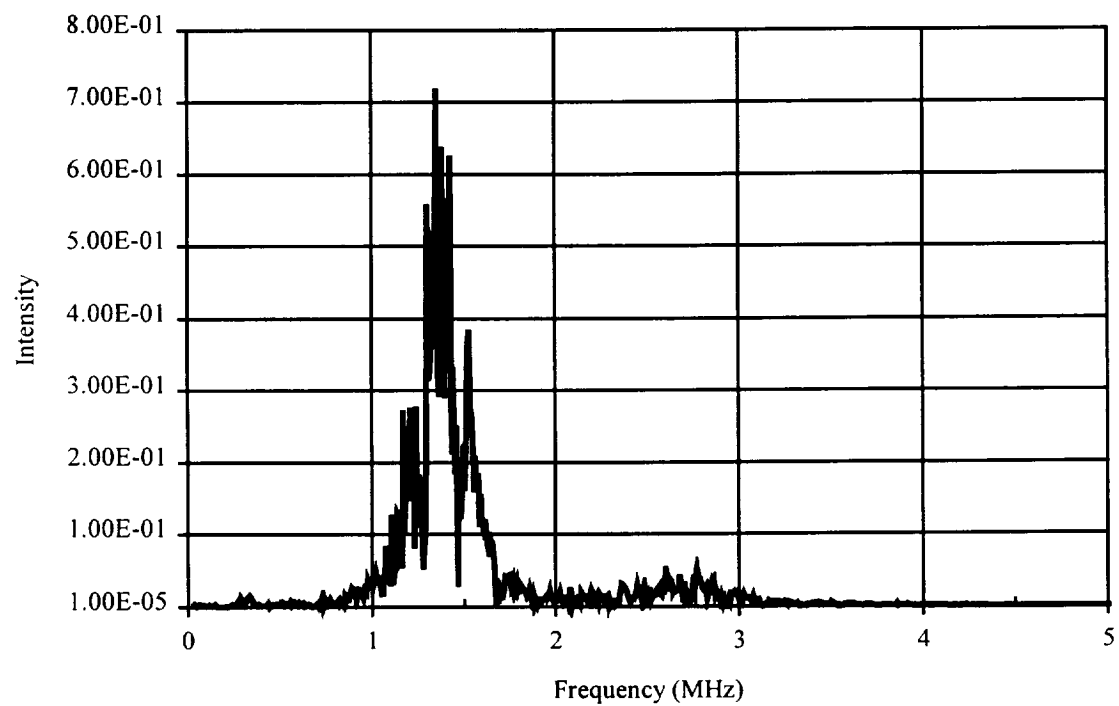
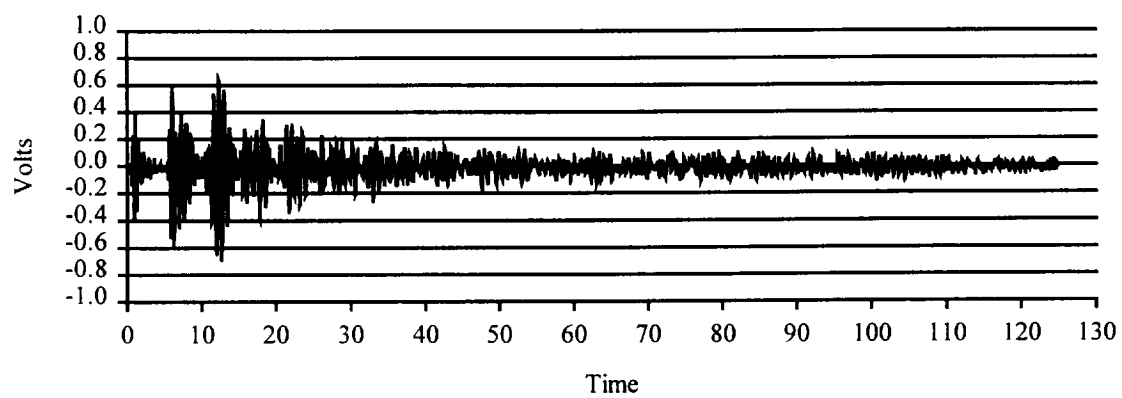
Pulser: AEROTECH 5.0 MHz (ENERGY = 1.0, Damping = 0.5)

Medium: Aluminum bar 18" long, 0.5" diameter

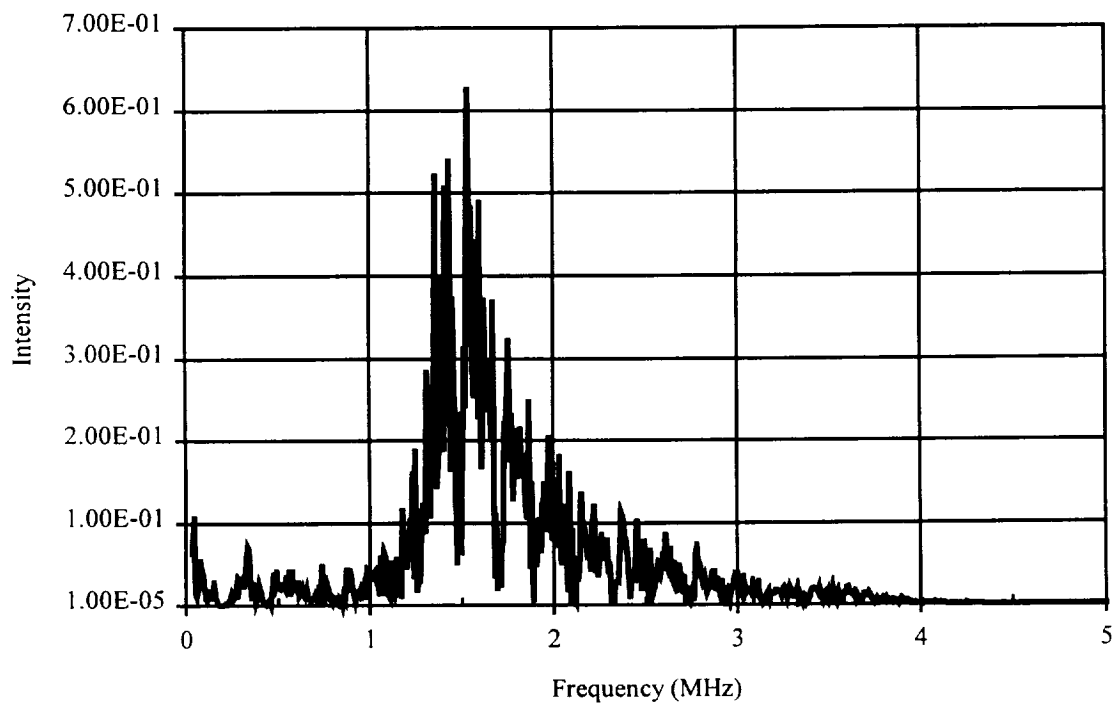
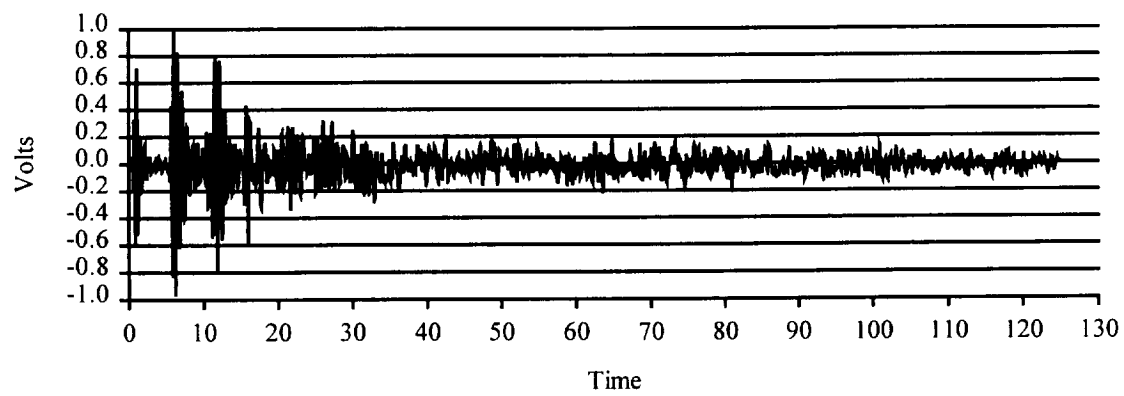
Configuration: End to end test, hot melt glue coupling



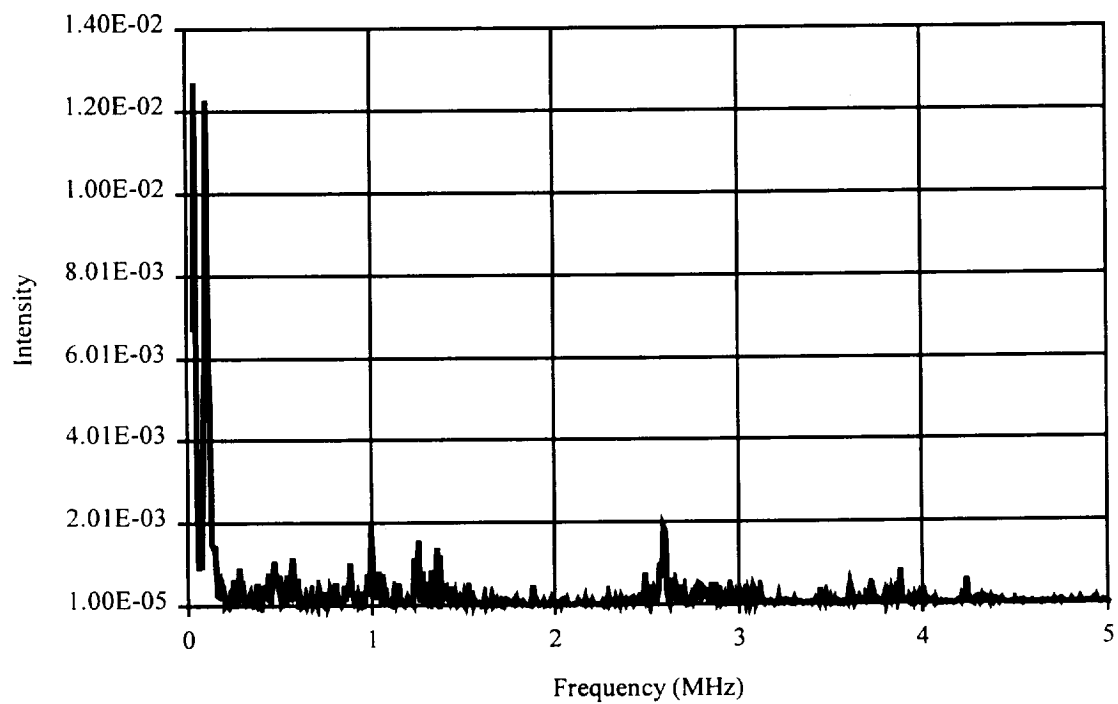
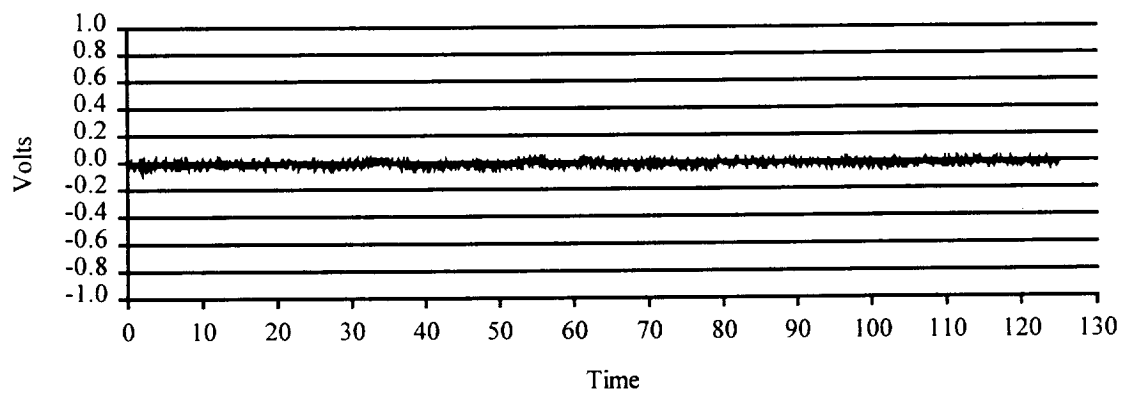
Transducer: CM-0204



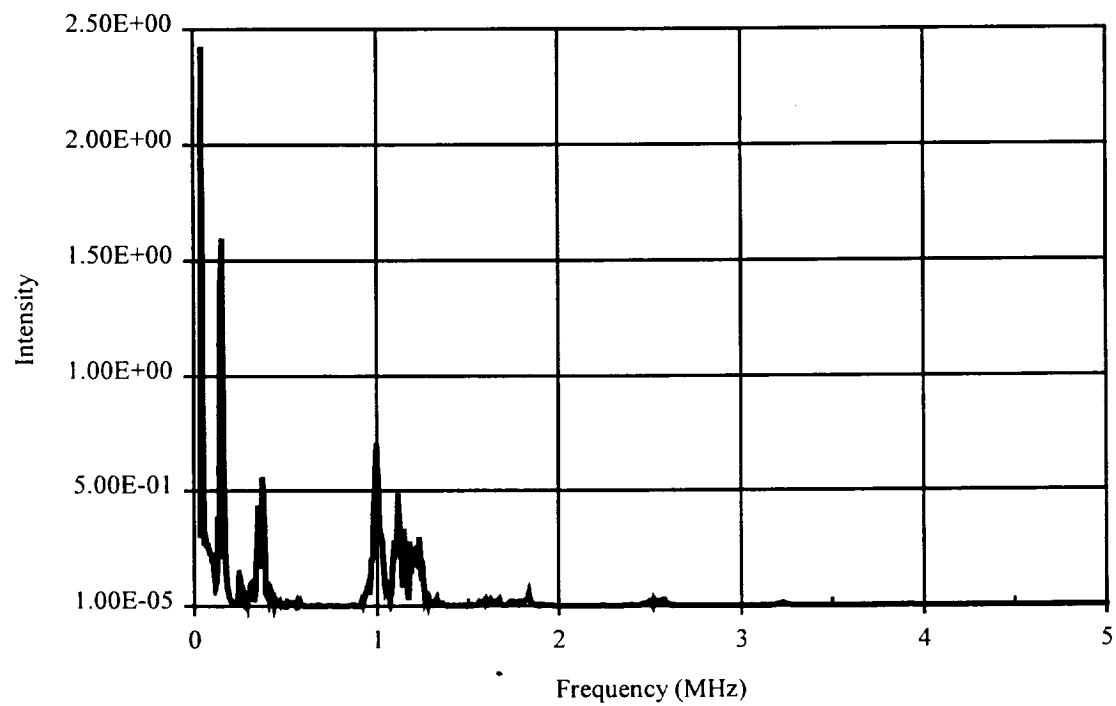
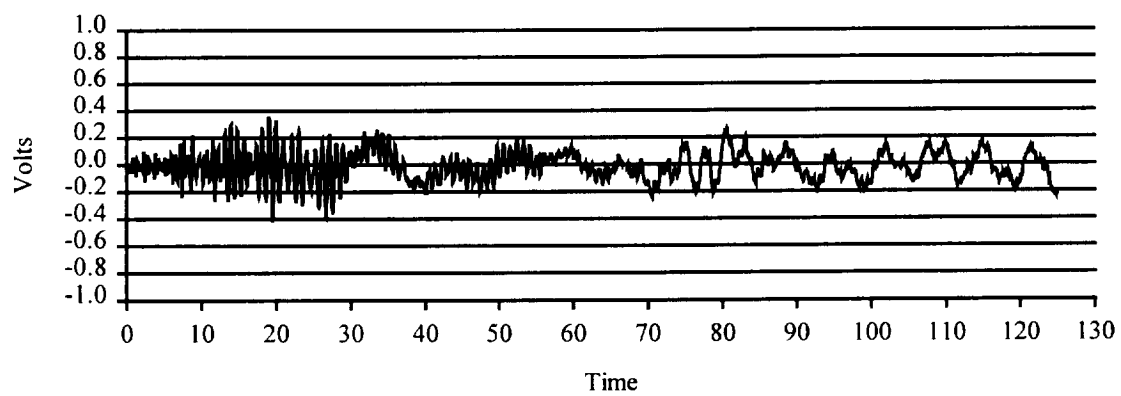
Transducer: Digital Wave B-1025



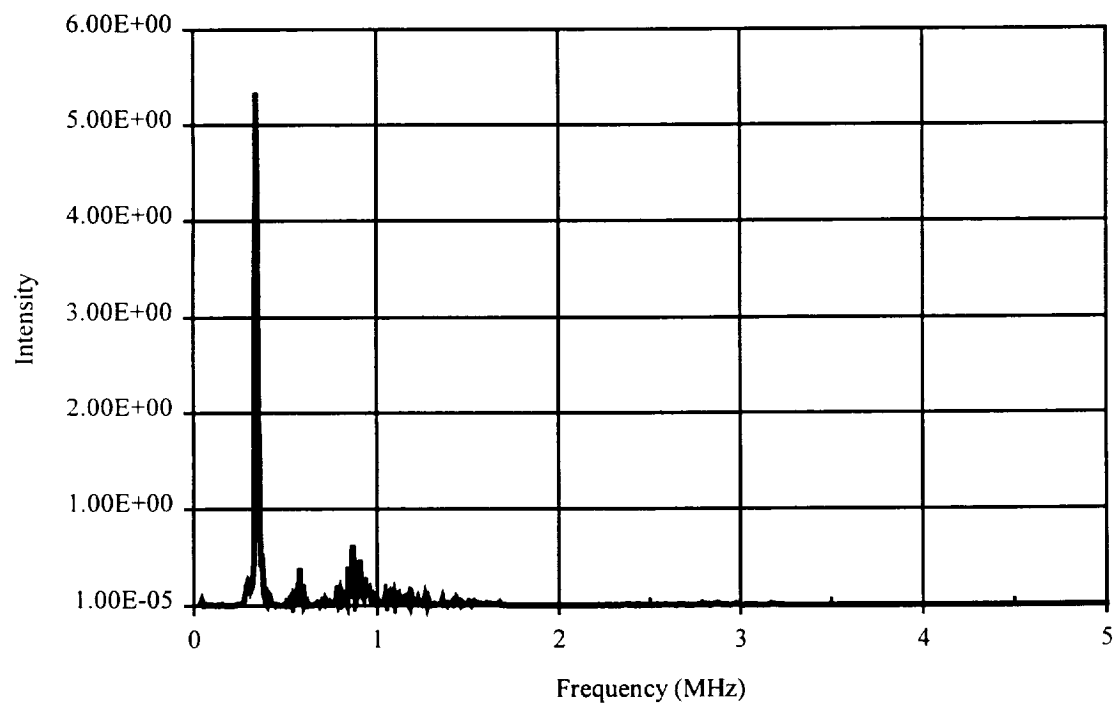
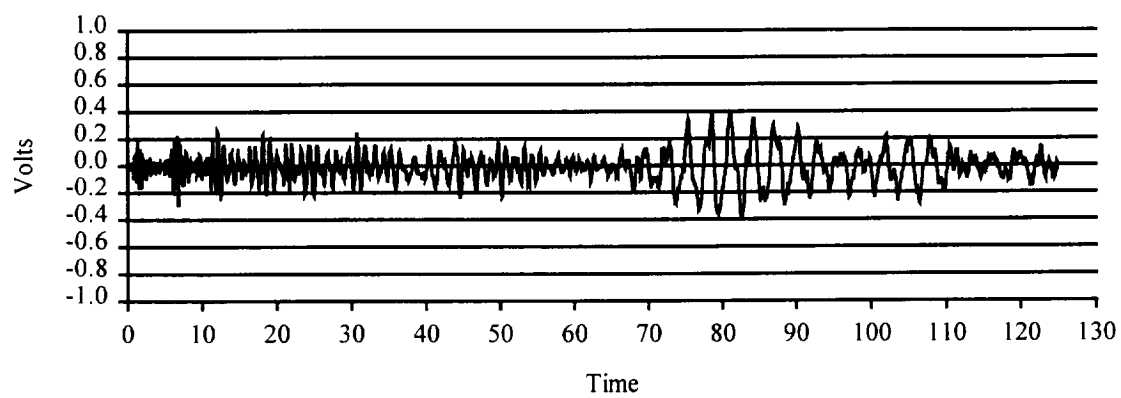
Transducer: HAE-1004



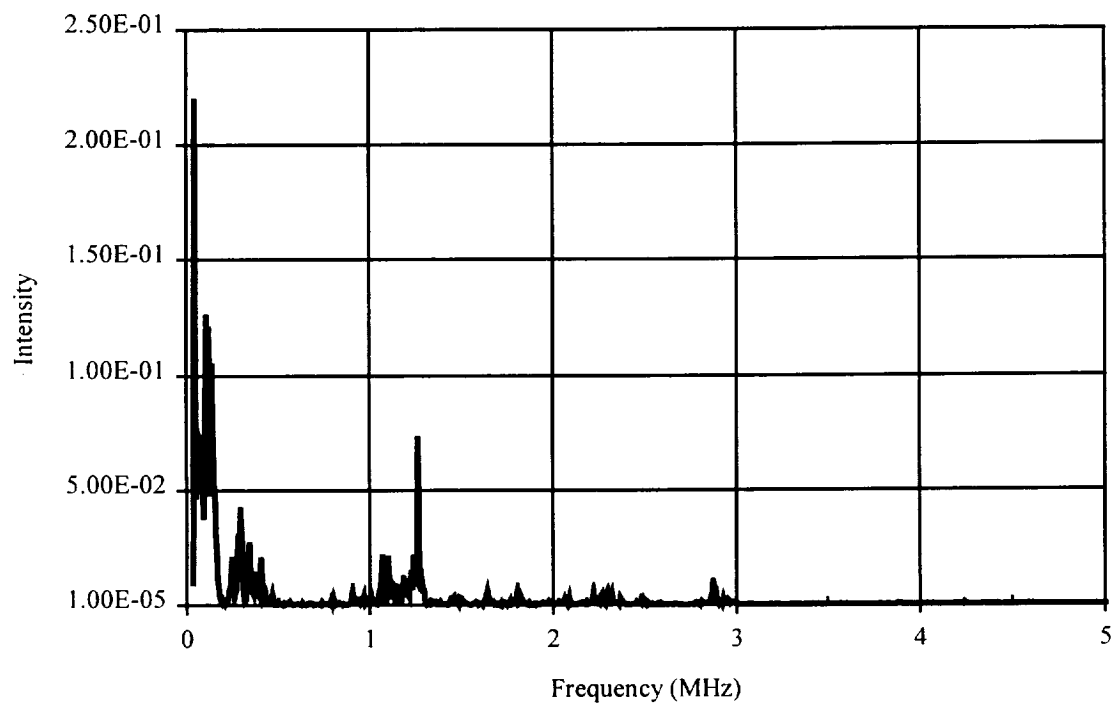
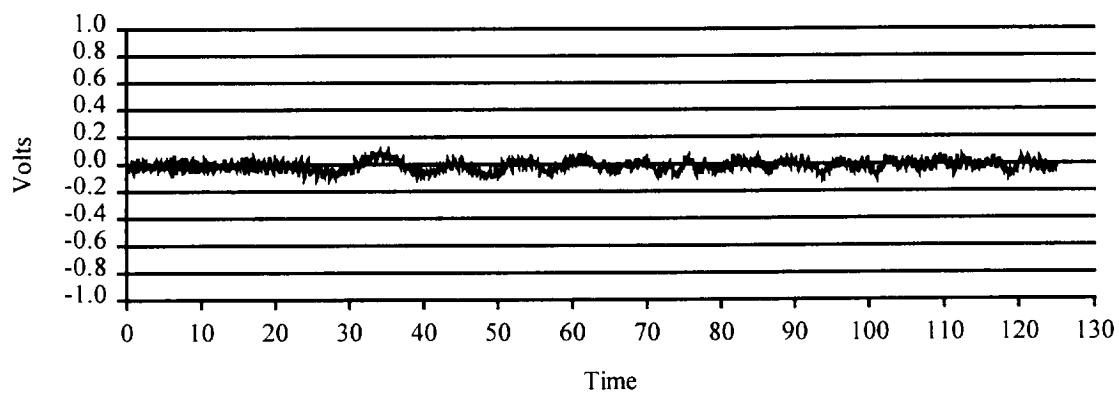
Transducer: Pyro



Transducer: R15



Transducer: R30



Transducer: S9208

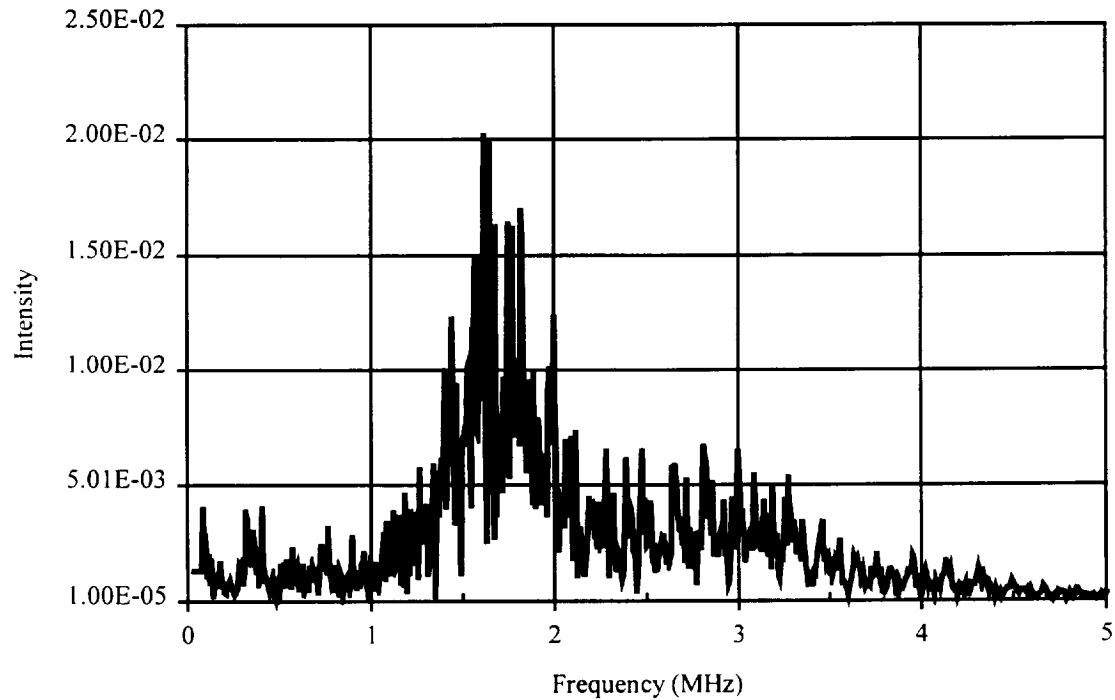
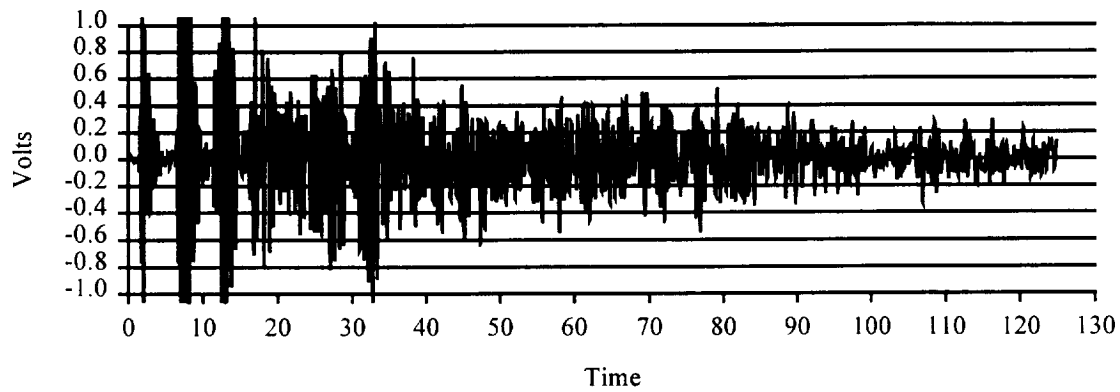
APPENDIX E

SIGNALS AFTER SECOND CRYOGENIC CYCLE

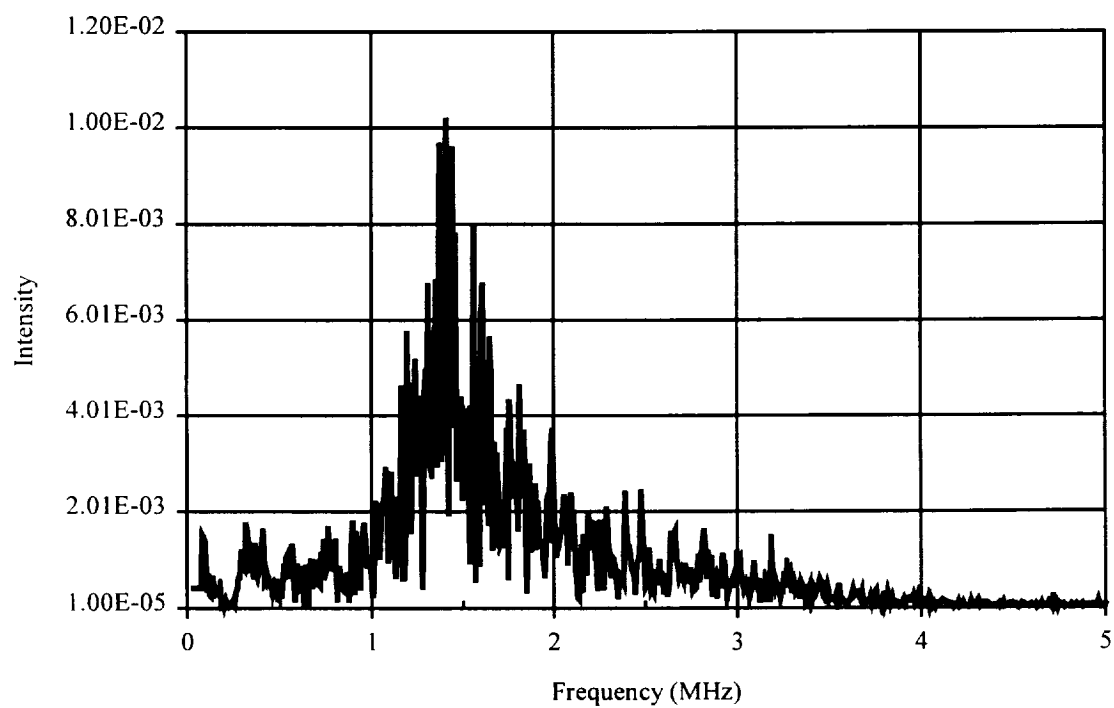
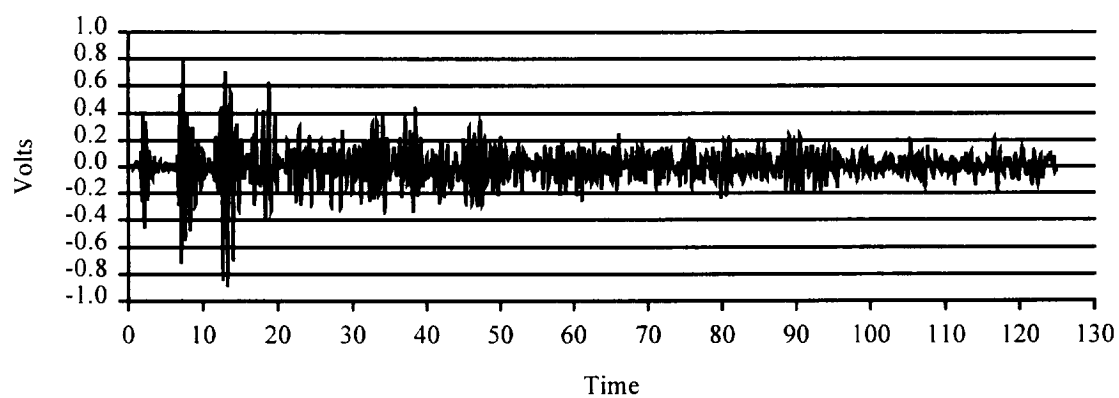
Pulser: AEROTECH 5.0 MHz (ENERGY = 1.0, Damping = 0.5)

Medium: Aluminum bar 18" long, 0.5" diameter

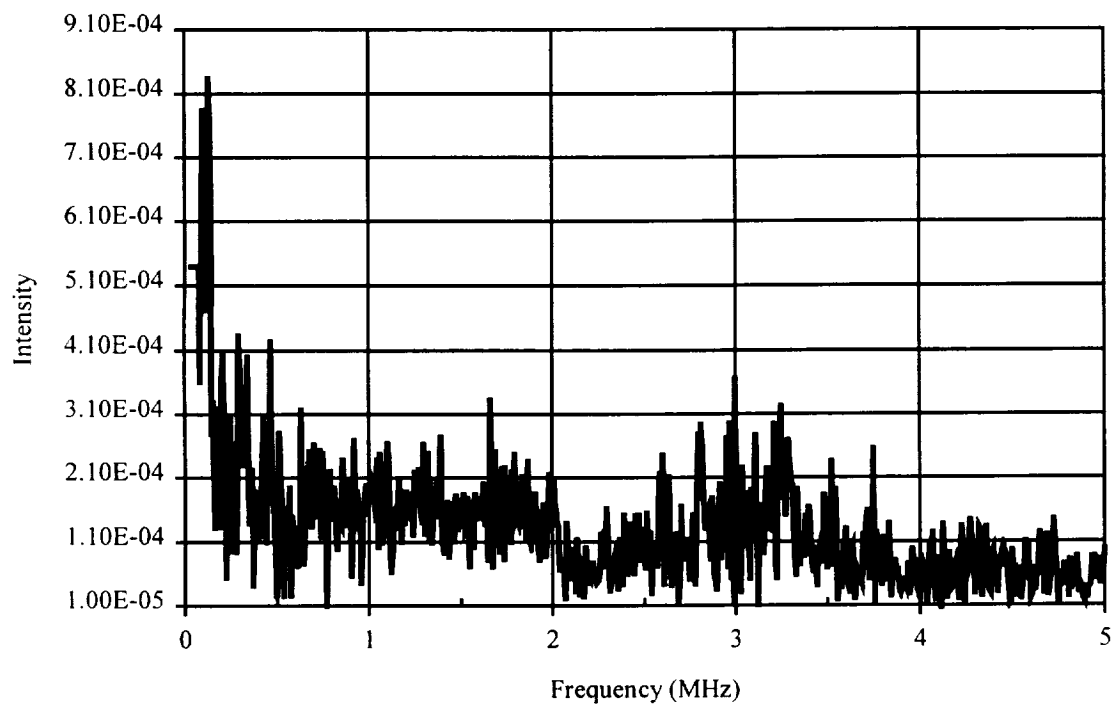
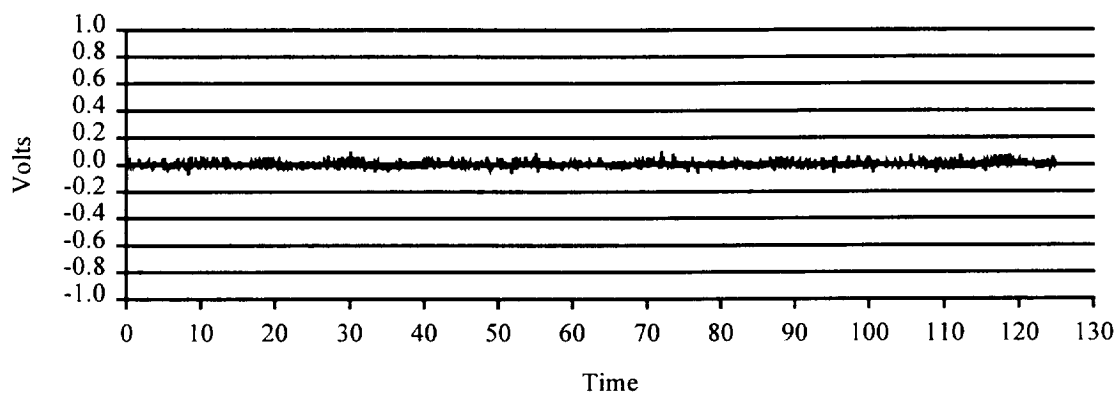
Configuration: End to end test, hot melt glue coupling



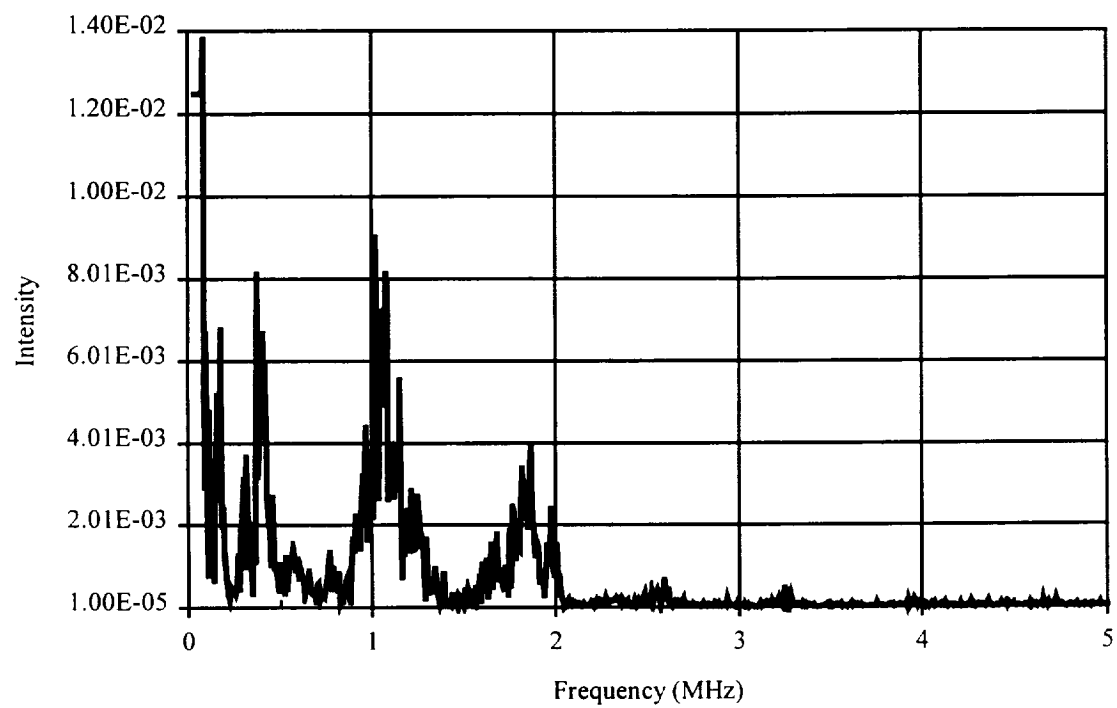
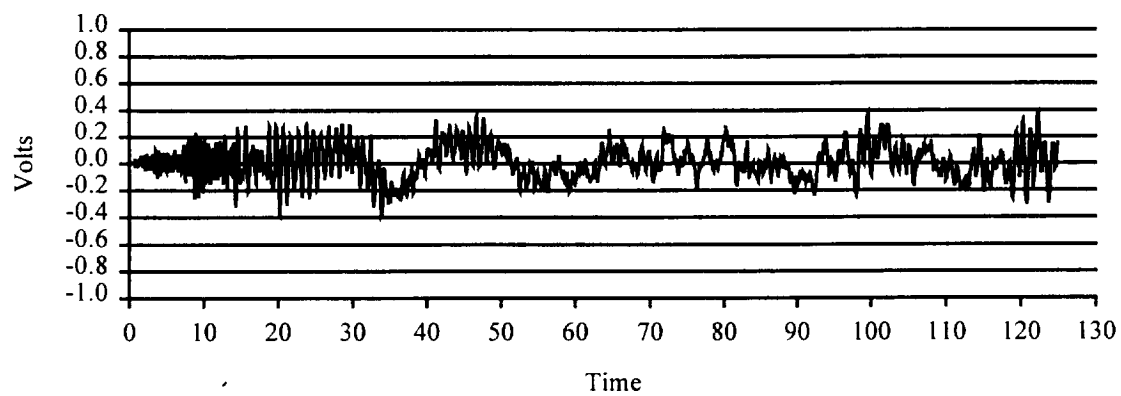
Transducer: CM-0204



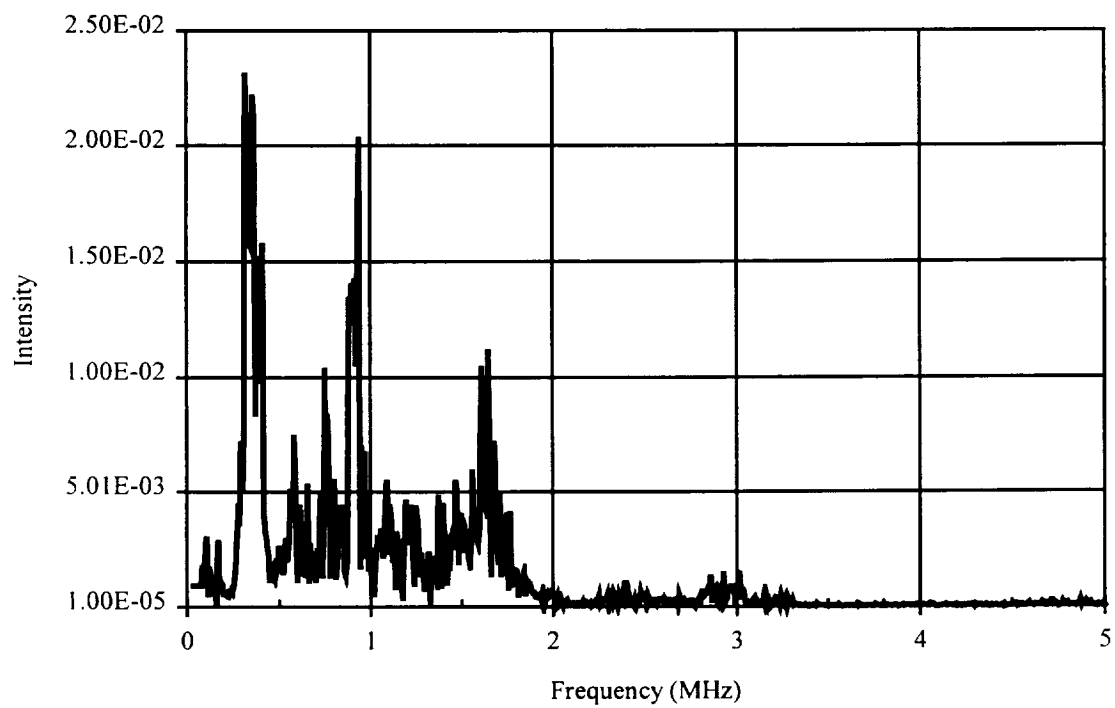
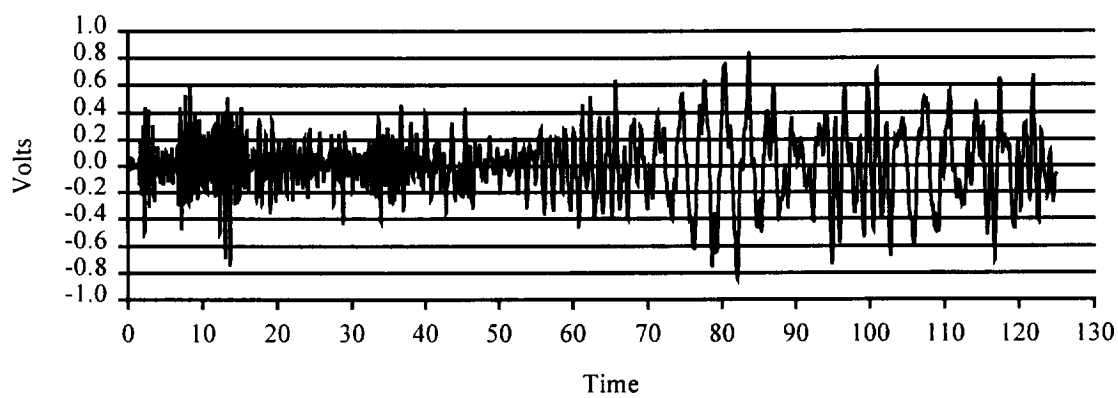
Transducer: Digital Wave B-1025



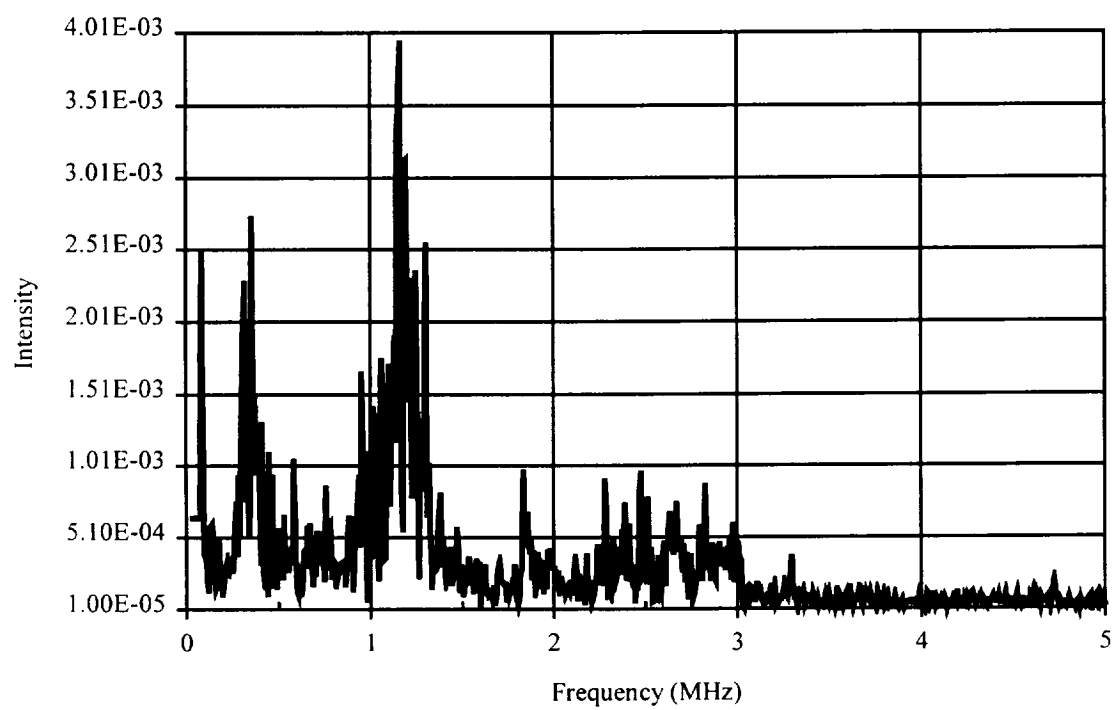
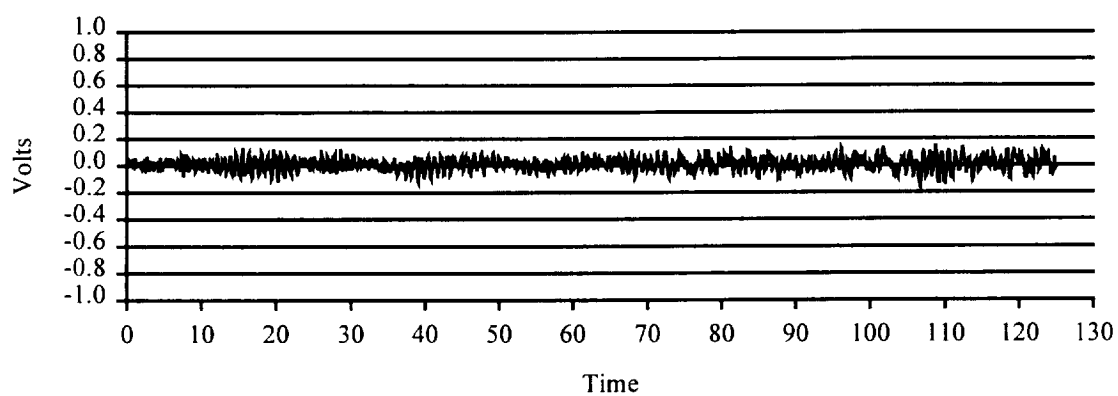
Transducer: S9215



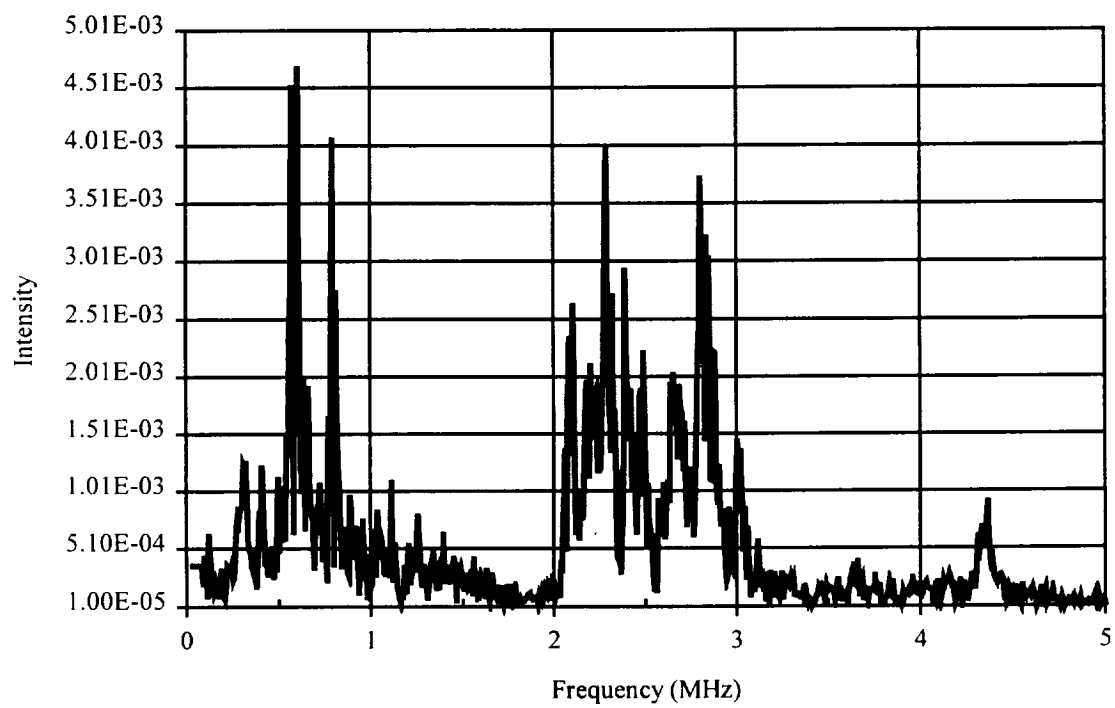
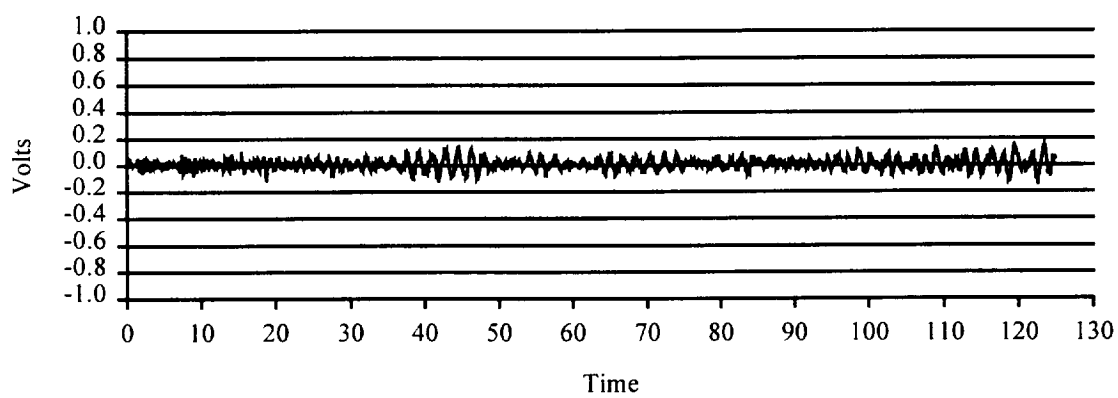
Transducer: R15



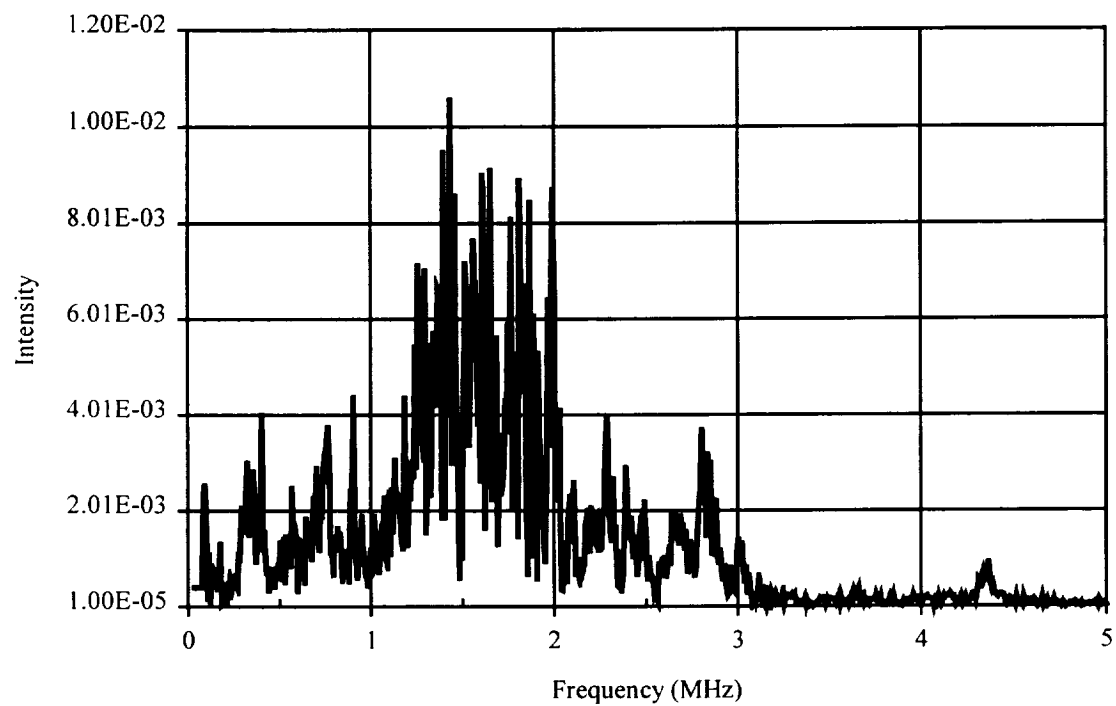
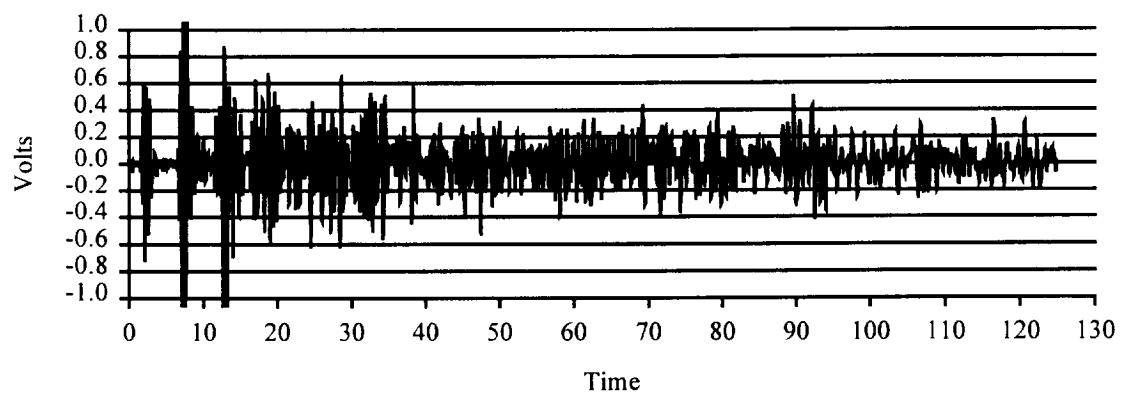
Transducer: R30



Transducer: S9208



Transducer: WD



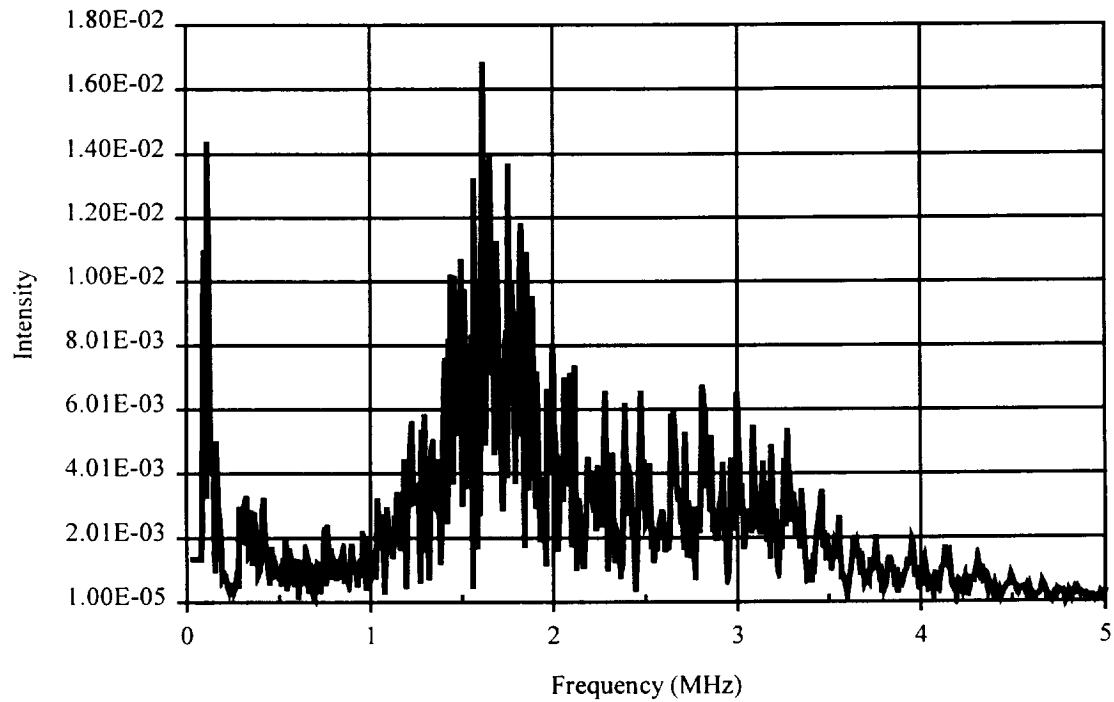
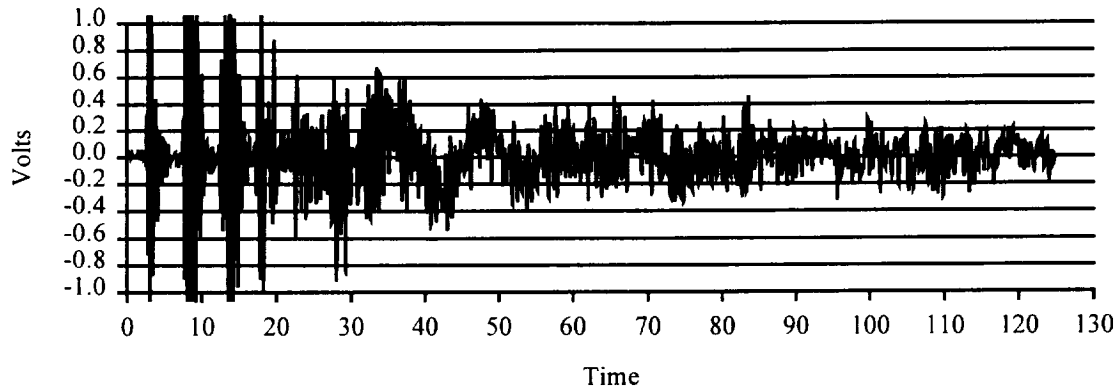
Transducer: HAE

APPENDIX F SIGNALS AFTER FIFTH CRYOGENIC CYCLE

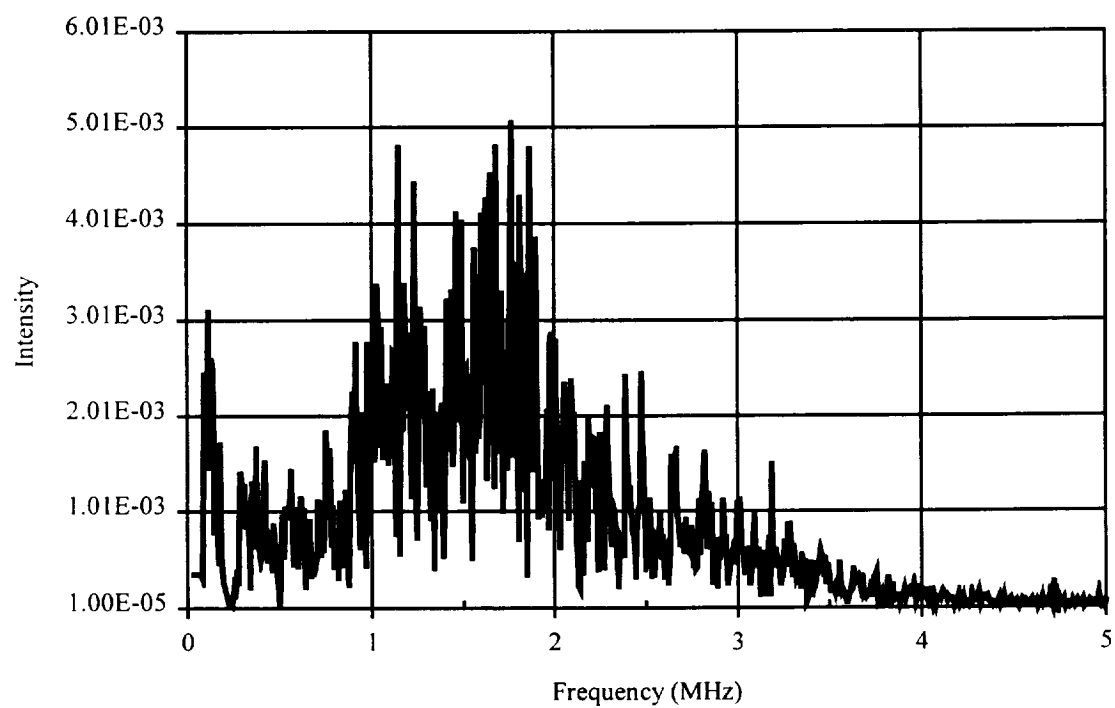
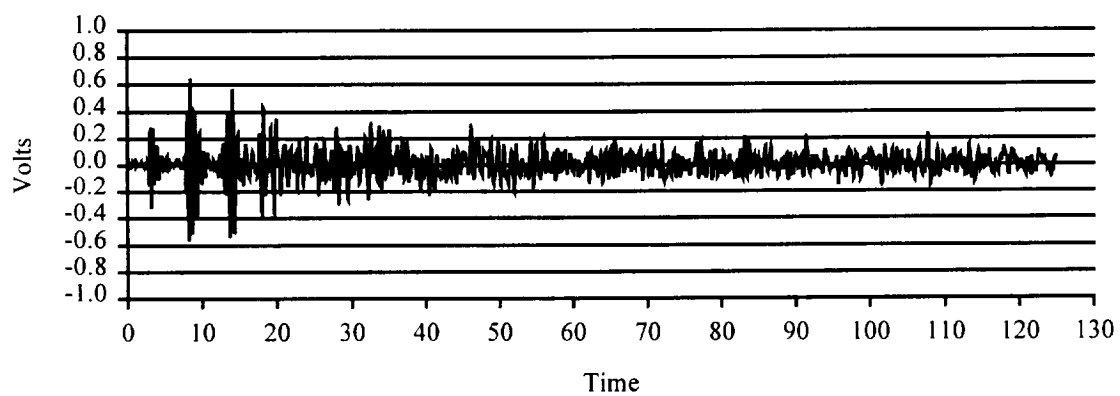
Pulser: AEROTECH 5.0 MHz (ENERGY = 1.0, Damping = 0.5)

Medium: Aluminum bar 18" long, 0.5" diameter

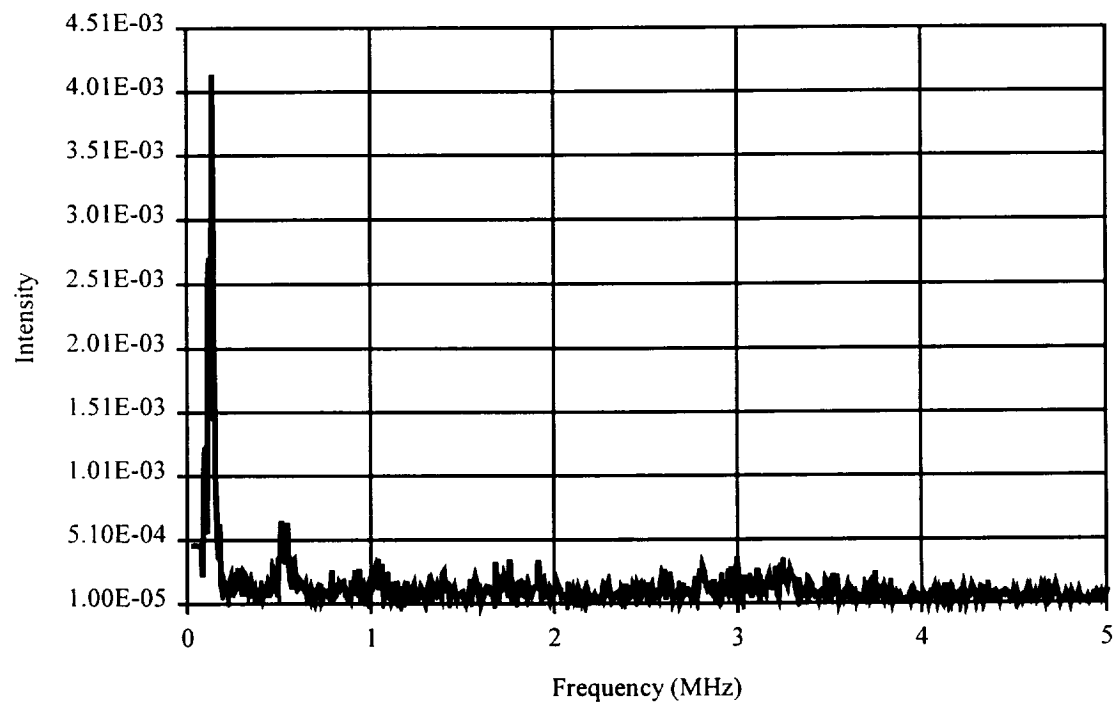
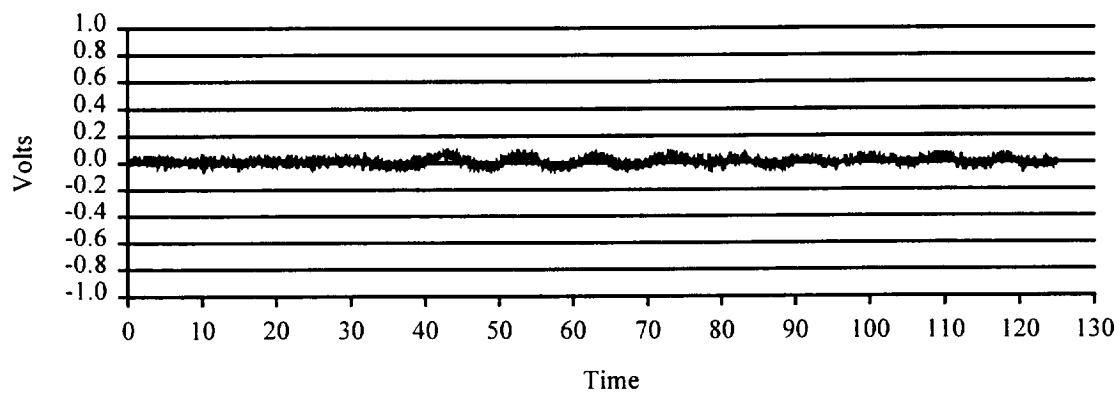
Configuration: End to end test, hot melt glue coupling



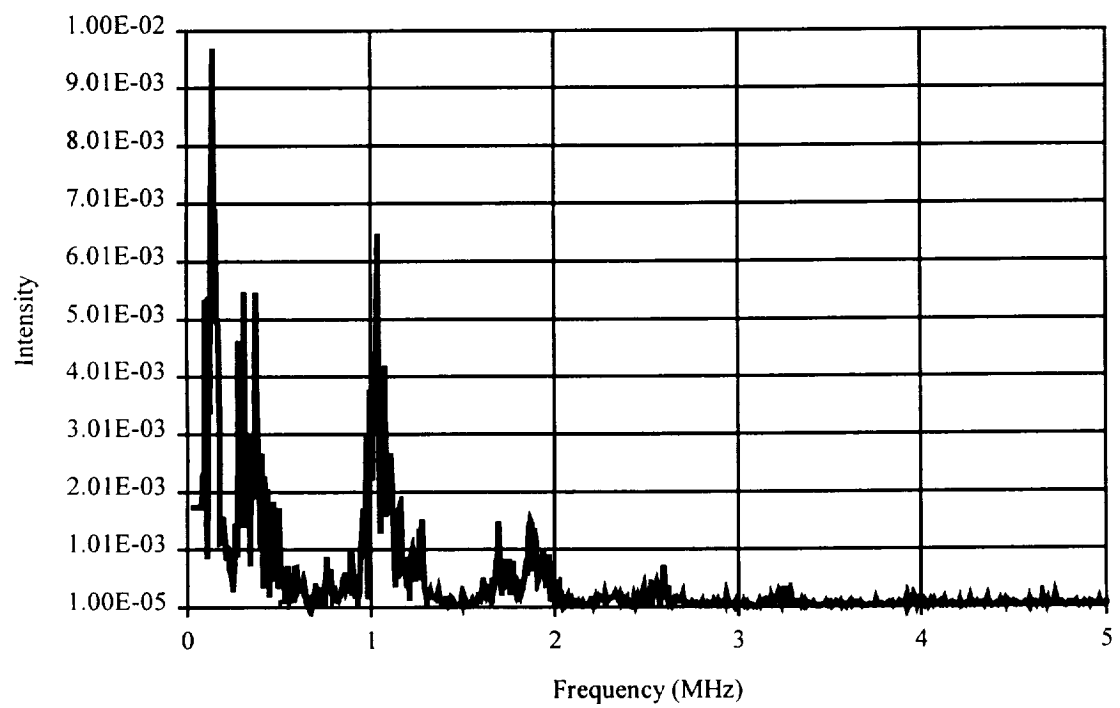
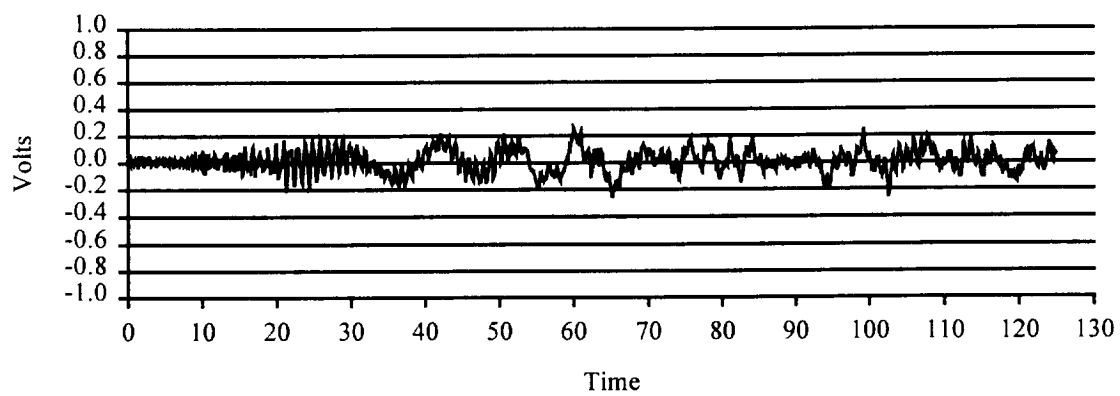
Transducer: CM-0204



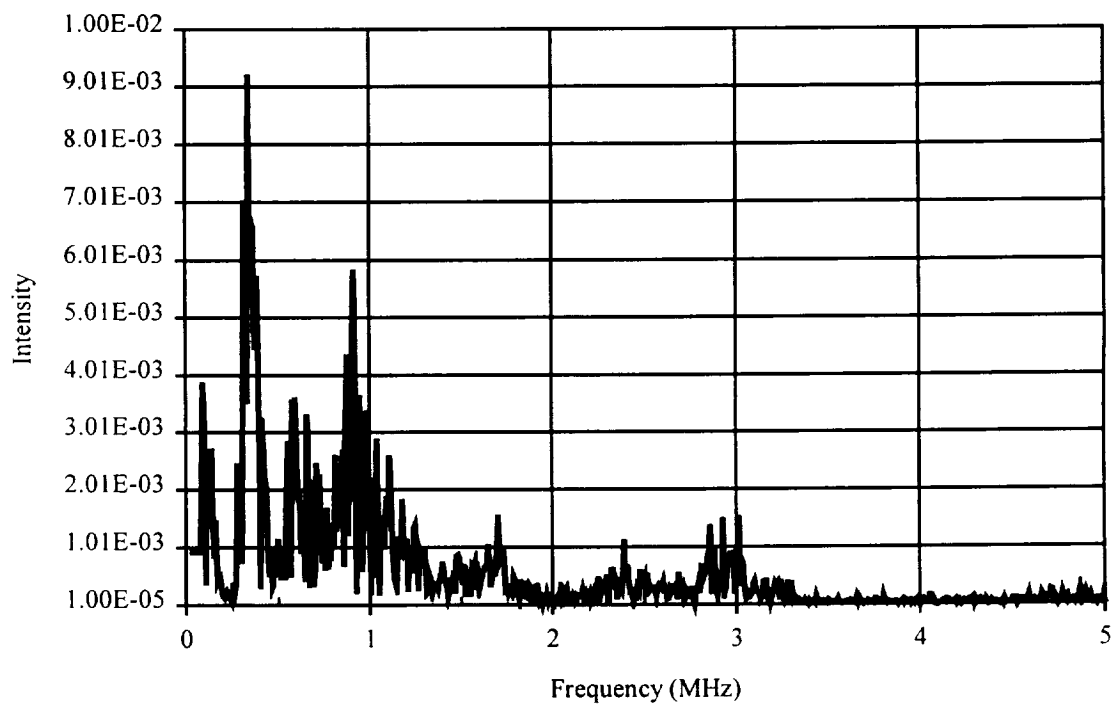
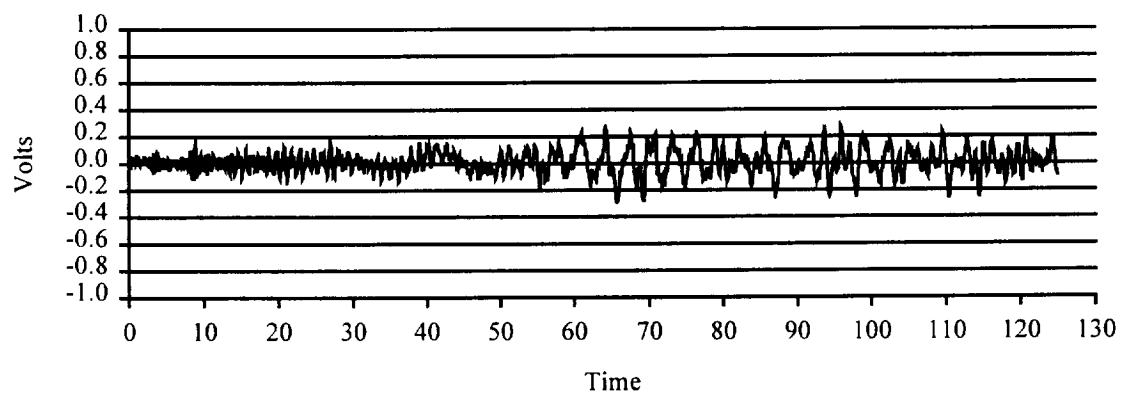
Transducer: Digital Wave B-1025



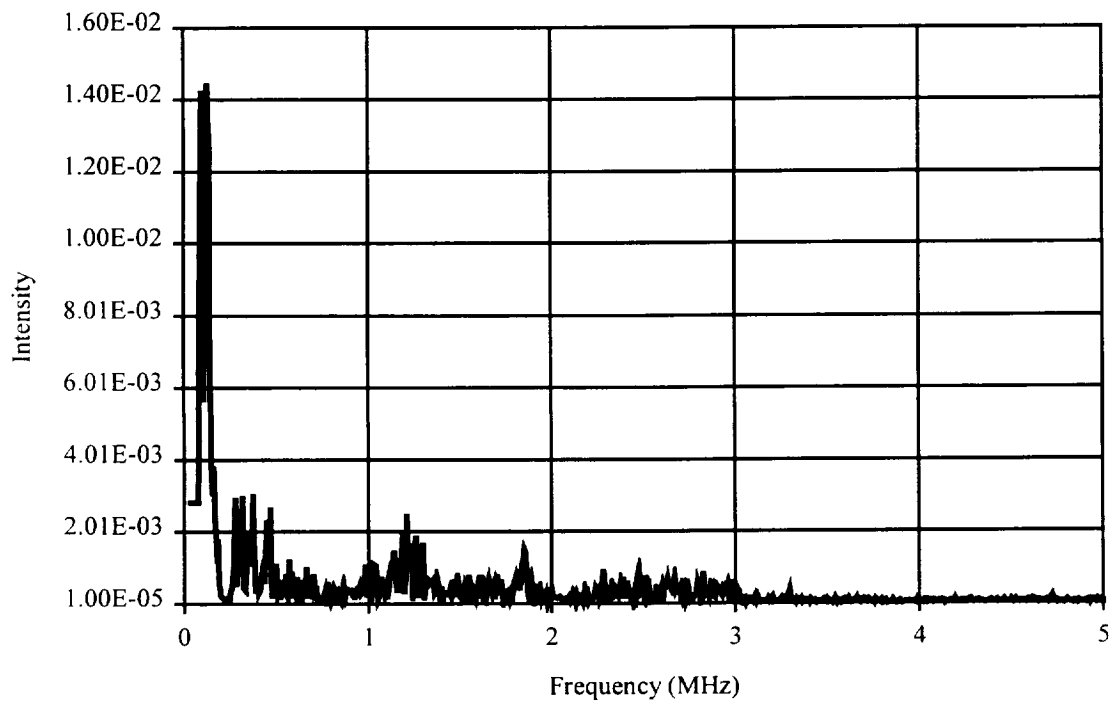
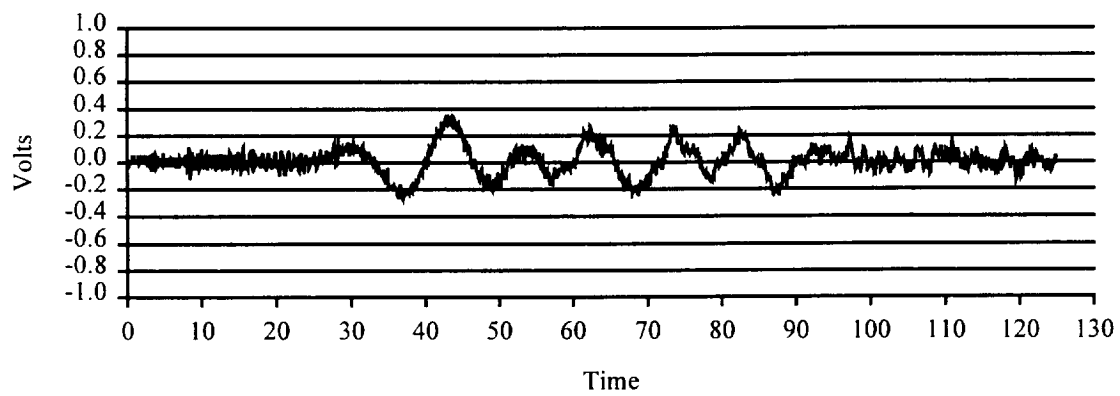
Transducer: S9215



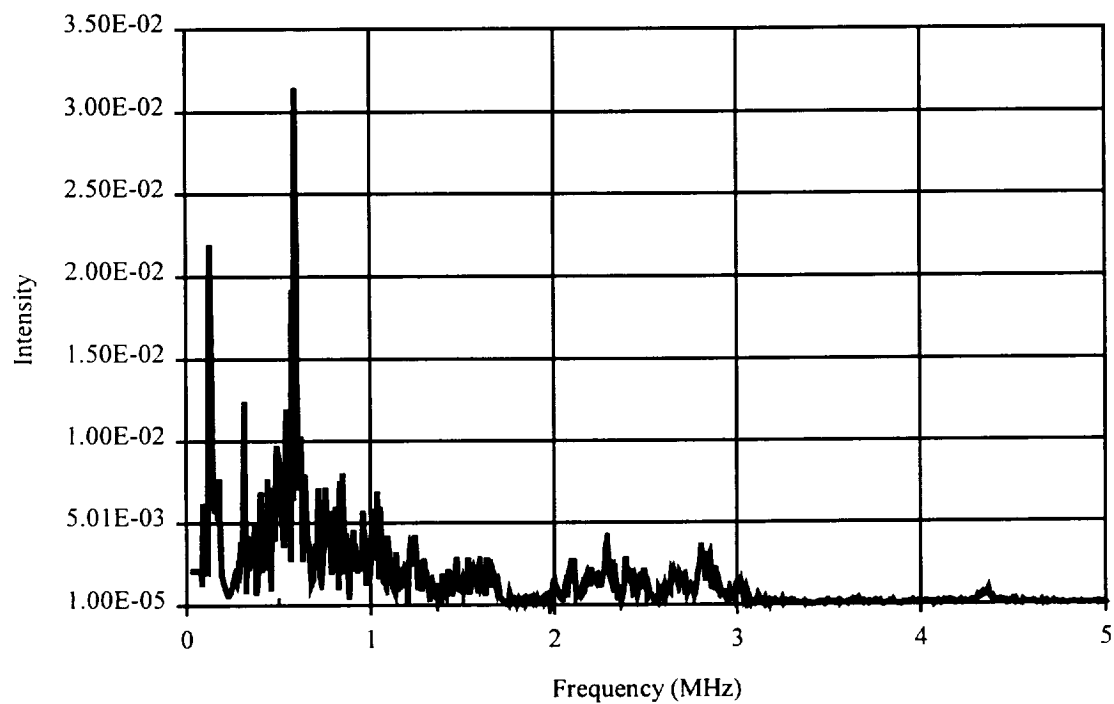
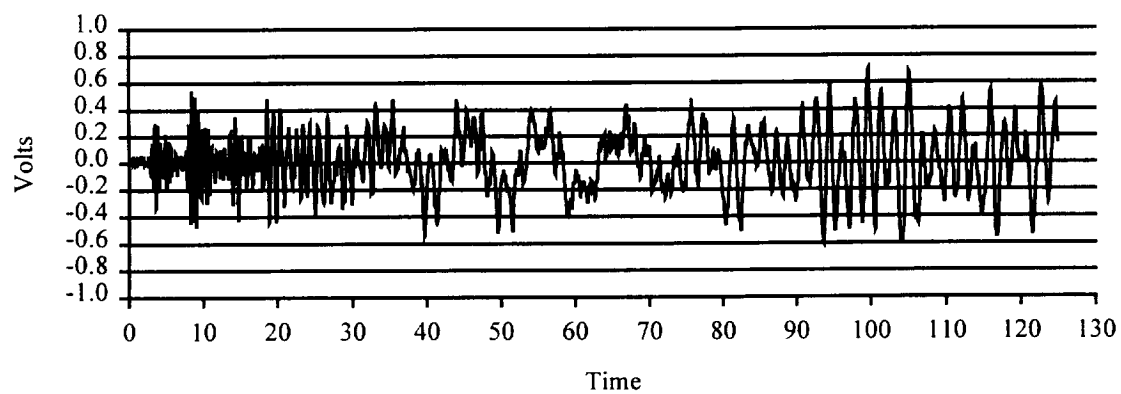
Transducer: R15



Transducer: R30



Transducer: S9208



Transducer: WD